Accepted Manuscript

Design, synthesis and evaluation of scutellarein-*O*-acetamidoalkylbenzylamines as potential multifunctional agents for the treatment of Alzheimer's disease

Zhipei Sang, Xiaoming Qiang, Yan Li, Rui Xu, Zhongcheng Cao, Qing Song, Ting Wang, Xiaoyu Zhang, Hongyan Liu, Zhenghuai Tan, Yong Deng

PII: S0223-5234(17)30320-3

DOI: 10.1016/j.ejmech.2017.04.054

Reference: EJMECH 9405

To appear in: *European Journal of Medicinal Chemistry*

Received Date: 26 January 2017

Revised Date: 27 March 2017

Accepted Date: 20 April 2017

Please cite this article as: Z. Sang, X. Qiang, Y. Li, R. Xu, Z. Cao, Q. Song, T. Wang, X. Zhang, H. Liu, Z. Tan, Y. Deng, Design, synthesis and evaluation of scutellarein-*O*-acetamidoalkylbenzylamines as potential multifunctional agents for the treatment of Alzheimer's disease, *European Journal of Medicinal Chemistry* (2017), doi: 10.1016/j.ejmech.2017.04.054.

Graphical abstract

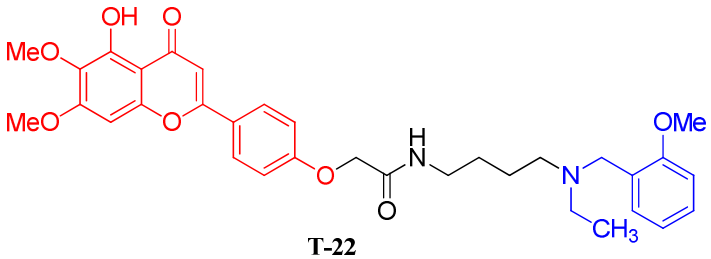

T-22

***Rat*AChE IC_{50}: 0.051 μM**	**Inhibition of self-induced Aβ_{1-42} aggregation: 57.1%**
***Hu*AChE IC_{50}: 0.039 μM**	**Inhibition of Cu^{2+}-induced Aβ_{1-42} aggregation: 43.4%**
Antioxidant (1.13 *eq* of Trolox)	**Inhibition of *Hu*AChE-induced Aβ_{1-42} aggregation: 57.3%**
Selective biometals chelator	**Disaggregation of Cu^{2+}-induced Aβ_{1-42} aggregation: 66.3%**
Low toxicity on SH-SY5Y cells	**Neuroprotective effect on H_2O_2 induced PC12 cell injury**

Reversed scopolamine-induced memory deficit in mice

Design, synthesis and evaluation of scutellarein-*O*-acetamidoalkylbenzylamines as potential multifunctional agents for the treatment of Alzheimer's disease

Zhipei Sang[a,b,#], Xiaoming Qiang[a,#], Yan Li[a], Rui Xu[a], Zhongcheng Cao[a], Qing Song[a], Ting Wang[a], Xiaoyu Zhang[a], Hongyan Liu[a], Zhenghuai Tan[c,*], Yong Deng[a,*]

[a]*Department of Medicinal Chemistry, Key Laboratory of Drug Targeting and Drug Delivery System of the Education Ministry, West China School of Pharmacy, Sichuan University, Chengdu, 610041, China*

[b]*College of Chemistry and Pharmaceutical Engineering, Nanyang Normal University, Nanyang, 473061, China*

[c]*Institute of Traditional Chinese Medicine Pharmacology and Toxicology, Sichuan academy of Chinese Medicine Sciences, Chengdu, 610041, China*

Abbreviations: AD, Alzheimer's disease; AChE, acetylcholinesterase; ACh, acetylcholine; A*β*, *β*-amyloid; APP, amyloid precursor protein; ROS, reactive oxygen species; MTDLs, multitarget-directed ligands; BuChE, butyrylcholinesterase; *Hu*AChE, human AChE; *Ee*AChE, *Electrophorus electricus* AChE; PDB, Protein Data Bank; *Tc*AChE, *Torpedo californica* AChE; CAS, catalytic active site; PAS, peripheral anionic site; ORAC-FL, Oxygen Radicals Absorbance Capacity by Fluorescence; ThT, thioflavin T; MTT, 3-(4,5-dimethylthiazol-2-yl)-2,5-diphenyltetrazolium; TMS, tetramethylsilane; HPLC, high-performance liquid chromatography; PBS, phosphate-buffered saline; DTNB, 5,5'-dithiobis-2-nitrobenzoic acid; ADT, Autodock Tools; AAPH, 2,2'-Azobis (amidinopropane) dihydrochloride; HFIP, 1,1,1,3,3,3-hexafluoro-2-propanol; HEPES, 4-(2-Hydroxyethyl)-1- piperazineethanesulfonic acid.

# These authors contributed equally to this work.

** Corresponding Author*.

Phone, +86-28-85258982; E-mail: tanzhh616@163.com (Zhenghuai Tan)

Phone, +86-28-85503790; E-mail: dengyong@scu.edu.cn (Yong Deng)

Abstract

A series of scutellarein-*O*-acetamidoalkylbenzylamines derivatives were designed based on a multitarget-directed ligands strategy for the treatment of Alzheimer's disease. Among these compounds, compound **T-22** demonstrated excellent acetylcholinesterase inhibitory, moderate inhibitory effects on self-induced A$\beta_{1\text{-}42}$ aggregation, Cu^{2+}-induced A$\beta_{1\text{-}42}$ aggregation, human AChE-induced A$\beta_{1\text{-}40}$ aggregation and disassembled Cu^{2+}-induced aggregation of the well-structured A$\beta_{1\text{-}42}$ fibrils, and also acted as potential antioxidant and biometals chelator. Both kinetic analysis of AChE inhibition and molecular modeling study suggested that **T-22** interacted with both the catalytic active site and peripheral anionic site of AChE. Moreover, compound **T-22** showed a good neuroprotective effect against H_2O_2-induced PC12 cell injury and low toxicity in SH-SY5Y cells. Furthermore, the step-down passive avoidance test indicated **T-22** significantly reversed scopolamine-induced memory deficit in mice. Taken together, the data showed that **T-22** was an interesting multifunctional lead compound worthy of further study for AD.

Keywords: Alzheimer's disease; Scutellarein-*O*-acetamidoalkylbenzylamines; Multifunctional agents; Acetylcholinesterase inhibitors; Aβ aggregation inhibitors; Antioxidant agents.

1. Introduction

Alzheimer's disease (AD) is the most common age related neurodegenerative disease, characterized by loss of cognitive ability, severe behavioral abnormalities, and ultimately death [1]. More than 47 million people worldwide suffered from AD, currently, and the figure is expecting to reach 131.5 million in 2050 [2]. Although the etiology of AD has not been completely known today, several factors including low levels of acetylcholine (ACh), oxidative stress, dyshomeostasis of biometals and *β*-amyloid (A*β*) deposits have been considered to play significant roles in the pathogenesis of AD [3-5].

ACh can be degraded by two types of cholinesterases, namely acetylcholinesterase (AChE) and butyrylcholinesterase (BuChE) [6]. AChE acts primarily as a regulatory enzyme at chlinergic synapses, while BuChE functionas as a co-regulator of cholinergic neurotransmission. Both Inhibition of acetylcholinesterase (AChE) and butyrylcholinesterase (BuChE) has been recognized as critical targets for the effective management of AD by increasing the availability of synaptic ACh in the brain regions [7]. However, BuChE is mainly localized in the peripheral tissues including plasma and very small amount is present in the brain region. Many side effects (*eg*. gastrointestinal events, nausea, vomiting, diarrhoea, dizziness) mainly associated with their peripheral AChE inhibitory activity [8]. Therefore, development of selective AChE inhibitors, with expectation of lesser peripheral inhibition of cholinesterase enzyme, may be a more suitable therapeutic strategy for the treatment of AD [9].

According to the amyloid hypothesis, the production and accumulation of oligomeric aggregates of A*β* in the brain are a central event in the pathogenesis of AD [10]. Aβ_{40} and Aβ_{42} are the main isoforms of A*β* peptides, are primarily produced depending on cleavage of amyloid precursor protein (APP) by *β*- and *γ*-secretases, respectively. Aβ_{42} is a major constituent of amyloid plaques and displays lower solubility and more toxic and has the tendency to form protofibrils and fibrillar aggregates at lower concentrations than Aβ_{40} [11]. Excess of metal ions such as Cu^{2+}, Fe^{2+}, Zn^{2+} and Al^{3+} have been found in A*β* plaques of AD brains, remarkably, Cu^{2+} and Zn^{2+} have been proved to promote A*β* aggregation as indicated previously [12]. Moreover, the abnormally high levels of redox-active metal ions such as Cu^{2+} and Fe^{2+} in brain might contribute to the overproduction of reactive oxygen species (ROS). Meanwhile, A*β* could enter the mitochondria where it would increase the generation of ROS and induce oxidative stress that damages biological molecules such as

proteins, DNA, and lipids [13]. Interestingly, oxidative stress promotes Aβ toxicity through the production of free radicals, and increases the generation of Aβ peptides, thus forming a vicious circle [14]. Noticeably, in accordance with "amyloid hypothesis", AChE produces secondary non-cholinergic functions that facilitate Aβ deposition in the form of senile plaques or neurofibrillary tangles in the brain [9].

The multifaceted factors of the AD have encouraged the development of multitarget-directed ligands (MTDLs) to act as agents for the treatment of this disease [15,16]. These drugs, which possess two or more complementary biological activities, may present significant clinical effectiveness in the future.

Scutellarin (4′,5,6-trihydroxyflavone-7-glucuronide), the major active component in breviscapine extracted from the Chinese herb *Erigeron breviscapus* (vant.) Hand.-Mazz., possesses a broad range of pharmacological properties related to neurological disorders, such as anti-inflammatory, antioxidant, neuroprotective and metal chelating properties [17,18]. Moreover, many researchers demonstrated that scutellarin can inhibit Aβ aggregation, attenuate Aβ-induced toxicity and reduce senile plaques [19]. However, scutellarin's poor solubility, low oral absorption and difficultly in passing through the blood–brain barrier restrict its clinical uses as an anti-AD drug [20]. Donepezil is approved by the FDA as an AChE inhibitor for the treatment of AD, the 1-benzylpiperidine fragment of donepezil has been shown as the cholinesterase inhibitory pharmacophore [21]. In addition, in our preliminary researches, the pharmacophore benzylamine that linked by alkylene is also required, which has suggested that this pharmacophore was directed toward peripheral anionic site of AChE by molecular modeling studies [22,23]. And the amide group could improve AChE inhibitory activities [24]. Therefore, in this paper, we aimed to use a multi-target-directed drug design strategy to combine 4′-hydroxy-5,6,7-trimethoxyflavone or 5,4′-dihydroxy-6,7-dimethoxyflavone with appropriate benzylamine fragments using amide linkers with different lengths. These new scutellarein-*O*-acetamidoalkylbenzylamines derivatives may simultaneously possess a dual binding site for AChE inhibition, anti-oxidative, metal chelating effects, neuroprotective properties, and inhibit Aβ aggregation.

In this study, a novel series of scutellarein-*O*-acetamidoalkylbenzylamines derivatives were designed, synthesized and evaluated for their biological activities, including inhibition of AChE and BuChE, the kinetics of enzyme inhibition, metal-chelating properties, antioxidant activities, effects

on Aβ aggregation and disaggregation, cytotoxic effects on SH-SY5Y cells, protective effect against H_2O_2-induced PC12 cell injury, and neuroprotective effects in the mouse scopolamine model of memory impairment. The chemical design strategy for scutellarein-*O*-acetamidoalkylbenzylamines derivatives is depicted in **Figure. 1**

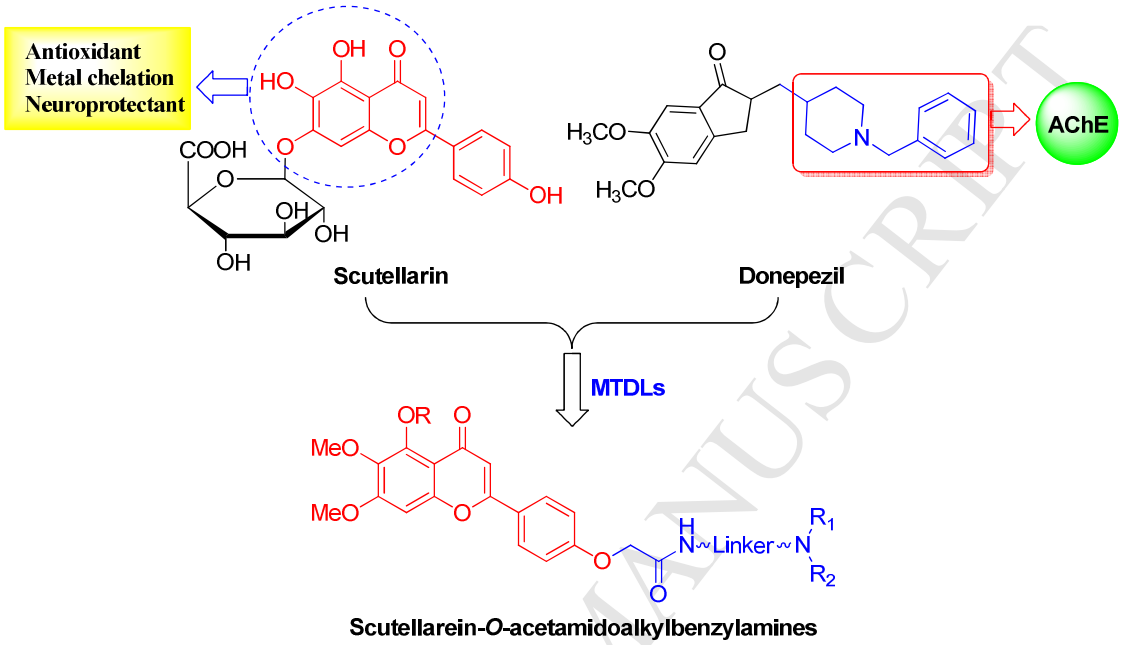

Figure 1. Design strategy for the scutellarein-*O*-acetamidoalkylbenzylamines derivatives.

2. Result and discussion

2.1. Chemistry

The synthetic route for the target compounds was shown in **Scheme 1**. Firstly, the starting material **1** was treated with excessive amounts of 1,2-dibromoethane, 1,3-dibromopropane, 1,4-dibromobutane or 1,6-dibromohexane in the presence of K_2CO_3 in anhydrous acetone under reflux to give the compounds **2a-d**. The key intermediates secondary amines **3a-d** were obtained according to the previous literature procedure in our lab [23]. Compounds **4-7** were obtained by the reaction of intermediates **2a-d** with **3a-d** in the presence of K_2CO_3 in anhydrous CH_3CN. Then, the key primary amines **8-11** were synthesized through the hydrazinolysis of **4-7**. On the other hand, the *p*-hydroxybenzaldehyde was treated with chloromethyl methyl ether to obtain 4-(methoxymethoxy)benzaldehyde (**13**) which was reacted with material **12** in the presence of 50% KOH to afford the key intermediate **14**, and then hydrolyzed with 10% HCl to obtain compound **15**. Compound **16** was prepared by the reaction of compound **15** with KI in the presence of *conc*.H_2SO_4,

removal of 5-methyl at flavonoid nucleus by anhydrous $AlCl_3$ in CH_3CN at 55–60°C gave the corresponding 5-OH scutellarein derivative **17**. Compounds **18a-b** was obtained by the reaction of **16** or **17** with ethyl bromoacetate in the presence of K_2CO_3, and then hydrolyzed with 30% LiOH and acidizing with 10% HCl to furnish the intermediates **19a-b**. Finally, condensation of compounds **19a-b** with the appropriate diamines **8-11** in the presence of EDCI in THF gave the target products **T-1~24**.

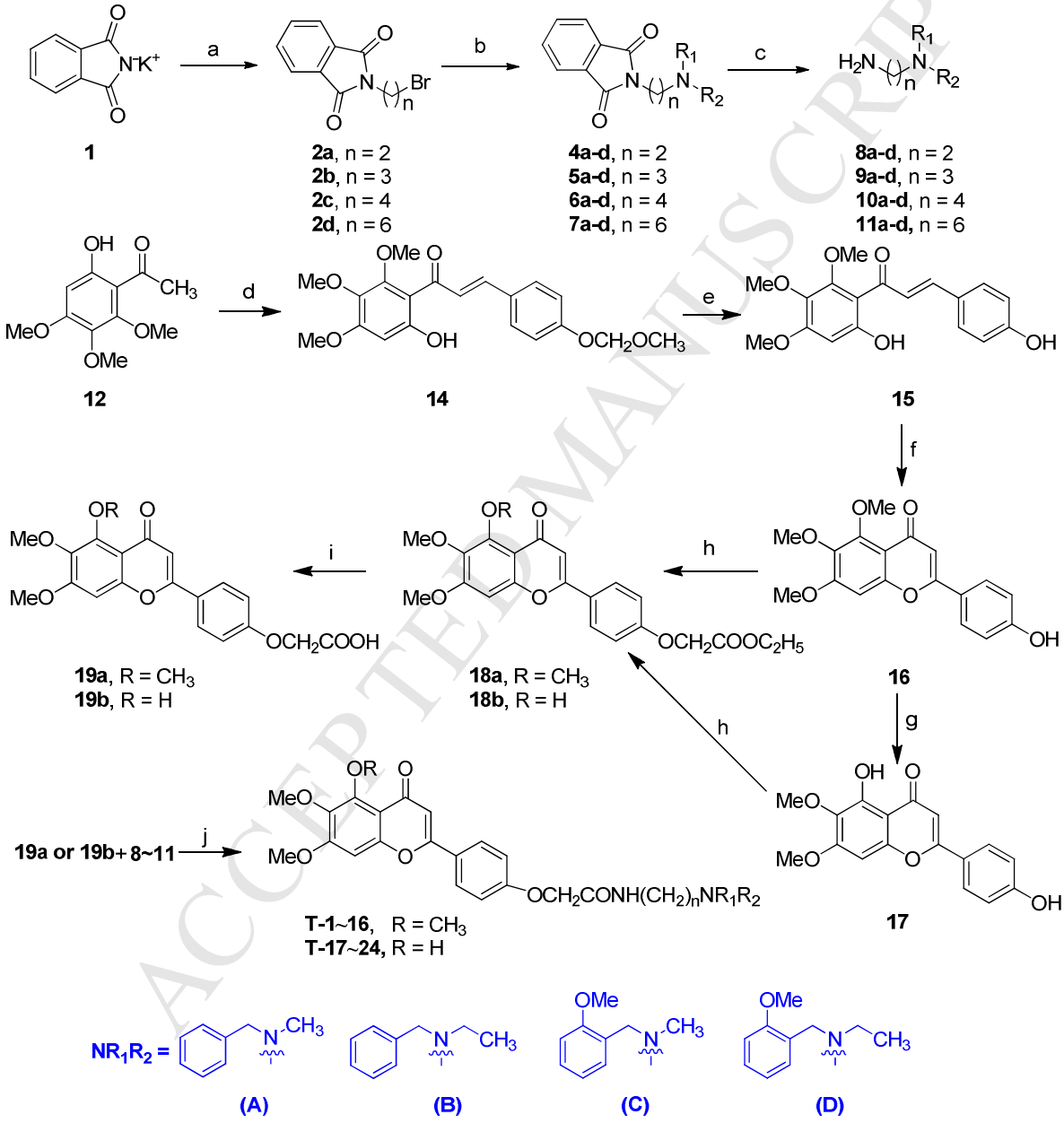

Scheme 1. Synthesis of scutellarein-*O*-acetamidoalkylbenzylamines derivatives **T-1~24**. *Reagents and conditions:* (a) $Br(CH_2)_nBr$, K_2CO_3, acetone, reflux, 7-8 h; (b) R_1R_2NH (**3a-d**)[21], K_2CO_3, CH_3CN, 65°C, 6-8 h; (c) $H_2NNH_2{\cdot}H_2O$, EtOH, reflux for 5 h; (d) *p*-MOM-O-PhCHO (**13**), 30% KOH, ethanol,

at r.t. for 3 days; (e) 10% HCl, ethanol, 50°C, 4 h; (f) KI, *conc*.H_2SO_4, DMSO, 100°C, 3-5 h; (g)$AlCl_3$, anhydrous CH_3CN, 60°C, 1 h; (h) $BrCH_2COOC_2H_5$, K_2CO_3, anhydrous CH_3CN, 65°C, 8 h; (i) LiOH, THF/H_2O, reflux for 2 h, then 10% HCl; (j) EDCI, THF, at r.t. for over night.

2.2. Pharmacology

2.2.1. Inhibition of AChE and BuChE

Inhibitory activities toward AChE and BuChE of the synthetic compounds were evaluated according to the modified Ellman's method [22]. Their activities were initially assayed on AChE from rat cortex homogenate and BuChE from rat serum. Moreover, the compounds were evaluated using *electric eel* AChE(*Ee*AChE) (**Table 1**), and the representative compounds were rationally selected and re-evaluated using human erythrocyte AChE (*Hu*AChE) (**Table 2**). In the above experiments, donepezil was used as reference compound and parent compounds **16** and **17** were also evaluated for comparative purposes. The IC_{50} values and selectivity index for the inhibition of AChE and BuChE were summarized in **Table 1**. As shown in **Table 1**, all the target compounds showed moderate to good AChE inhibitory activity and acted as highly selective AChE inhibitors. Compound **T-22** displayed the most potent inhibitory activity for AChE with IC_{50} value of 0.051 ± 0.003 μM, which was similar to donepezil (IC_{50} = 0.015 ± 0.002 μM). Almost all the target compounds showed weak activity against BuChE. Among them, compound **T-16** exhibited the most potent inhibitory activity for BuChE with IC_{50} value of 2.4 ± 0.01 μM.

In preliminary studies, as expected, the parent compounds **16** (IC_{50} > 500 μM) and **17** (IC_{50} > 500 μM) exhibited no significant inhibition of AChE. Introduction of benzylamines group increased the AChE inhibitory capacity and improved the selectivity for AChE over BuChE. Considering the potential role of BuChE in AD pathogenesis, this selectivity profile may be a limitation, but this also may be beneficial to diminish peripheral cholinergic side effects and provide lower toxicity [25]. Through analysis and comparison, we found that the properties of the substitutions at flavonoid nucleus 5 position showed significant influence on AChE inhibitory activities: 5-methoxy substituted derivatives (**T-3**, **T-4**, **T-7**, **T-8**, **T-15** and **T-16**) exhibited higher activity than that with 5-hydroxyl substituted (**T-17**, **T-18**, **T-19**, **T-20**, **T-23** and **T-24**), except compounds **T-11** and **T-12** with 5-methoxy (IC_{50} = 8.32 ± 0.21 μM and 0.074 ± 0.006 μM, respectively) exhibited much less potent

than corresponding compounds **T-21** and **T-22** with 5-hydroxyl (IC_{50} = 2.29 ± 0.02 μM and 0.051 ± 0.001 μM, respectively). The screening data also revealed that the structure of terminal groups NR_1R_2 of side chain affected inhibitory activities. Generally, the *N*-2-methoxybenzyl groups indicated stronger inhibitory potency than *N*-benzyl groups. And the compounds possessing a *N*-ethyl group showed obviously better AChE inhibitory activity than the compounds with a *N*-methyl group, which was consistent with the previously reported results in our lab [22,23]. On the other hand, we also investigated the effects of the side chain length on inhibitory ability of AChE, the optimal chain length was four-methylene linker. Finally, compound **T-22** showed the most potent inhibition for *Rat*AChE with an IC_{50} value of 0.051 ± 0.001 μM. For the inhibition of *Ee*AChE, it is notable that all the tested compounds exhibited a higher inhibitory activity towards *Rat*AChE than *Ee*AChE (**Table 1**). Furthermore, compounds **T-12, T-16, T-22** and **T-24**, which displayed the better potent inhibitory activity for *Rat*AChE (IC_{50} = 0.074 ± 0.006 μM, 0.35 ± 0.02 μM, 0.051 ± 0.001 μM and 0.37 ± 0.01 μM, respectively), were re-evaluated using *Hu*AChE (**Table 2**). The inhibitory activity against *Rat*AChE is lower than that against *Hu*AChE.

Table 1. Inhibition of AChE and BuChE activity, and oxygen radicals absorbance capacity (ORAC, Trolox Equivalents) by compounds **T-1~24**, **16**, **17** and donepezil.

Compound	R	n	$-NR_1R_2$	IC_{50} ± SD[a] (μM)			Selectivity index[e]	ORAC [f]
				*Rat*AChE[b]	*Rat*BuChE[c]	*Ee*AChE[d]		
T-1	CH_3	2	**A**	15.80 ± 0.46	>500	17.90 ± 0.56	>31.6	0.42eq
T-2	CH_3	2	**B**	0.58 ± 0.06	>500	16.20 ± 0.42	>862	0.39eq
T-3	CH_3	2	**C**	1.44 ± 0.08	110.0 ± 0.56	13.40 ± 0.51	76.4	0.40eq
T-4	CH_3	2	**D**	2.39 ± 0.04	65.4 ± 0.13	6.81 ± 0.19	27.4	0.42eq
T-5	CH_3	3	**A**	8.42 ± 0.32	>500	23.51 ± 1.05	>59.4	0.39eq
T-6	CH_3	3	**B**	3.28 ± 0.11	>500	18.56 ± 0.73	>152	0.38eq
T-7	CH_3	3	**C**	1.58 ± 0.03	>500	5.20 ± 0.11	>316	0.40eq
T-8	CH_3	3	**D**	0.24 ± 0.01	346.0 ± 1.26	6.63 ± 0.17	1442	0.33eq
T-9	CH_3	4	**A**	5.36 ± 0.22	>500	13.93 ± 0.32	>93.3	0.35eq
T-10	CH_3	4	**B**	0.76 ± 0.01	219.1 ± 2.13	14.38 ± 0.52	288	0.36eq
T-11	CH_3	4	**C**	8.32 ± 0.21	>500	18.40 ± 0.71	>60.1	0.37eq

T-12	CH_3	4	**D**	0.074 ± 0.006	>500	9.77 ± 0.34	>6757	0.38eq
T-13	CH_3	6	**A**	4.63 ± 0.12	117.7 ± 0.65	23.44 ± 0.96	25.3	0.37eq.
T-14	CH_3	6	**B**	2.84 ± 0.09	108.0 ± 0.78	33.24 ± 1.03	38.0	0.39eq.
T-15	CH_3	6	**C**	5.54 ± 0.17	130.0 ± 1.67	16.23 ± 0.68	23.5	0.41eq.
T-16	CH_3	6	**D**	0.35 ± 0.02	2.4 ± 0.01	17.65 ± 0.47	6.8	0.34eq.
T-17	H	2	**C**	1.97 ± 0.04	105.5 ± 0.69	14.03 ± 0.46	53.3	1.18eq.
T-18	H	2	**D**	4.98 ± 0.22	74.3 ± 0.57	14.11 ± 0.25	14.9	1.04eq.
T-19	H	3	**C**	2.59 ± 0.07	>500	15.50 ± 0.72	>193	1.14eq.
T-20	H	3	**D**	0.31 ± 0.01	>500	11.22 ± 0.11	>1613	0.97eq.
T-21	H	4	**C**	2.29 ± 0.02	178.0 ± 0.96	17.13 ± 0.58	77.7	0.97eq.
T-22	H	4	**D**	0.051 ± 0.001	>500	15.95 ± 0.39	>9804	1.13eq.
T-23	H	6	**C**	6.63 ± 0.02	>500	12.29 ± 0.47	>75.4	1.01eq.
T-24	H	6	**D**	0.37 ± 0.01	>500	11.67 ± 0.26	>1351	0.99eq.
16				>500	>500	NT[g]	----	1.86eq
17				>500	>500	NT[g]	----	3.07eq
Donepezil				0.015 ± 0.002	20.7 ± 1.36	0.027 ± 0.001	1380	NT[g]

[a] IC_{50} values represent the concentration of inhibitor required to decrease enzyme activity by 50% and are the mean of 3 independent experiments.

[b] From 5% rat cortex homogenate.

[c] BuChE from rat serum.

[d] From *electrophorus electricusc*.

[e] Selectivity index = IC_{50} (*Rat*BuChE)/IC_{50} (*Rat*AChE).

[f] Results are expressed as μM of Trolox equivalent/μM of tested compound.

[g] NT = not tested.

2.2.2. Kinetic characterization of AChE inhibition.

To investigate the AChE inhibitory mechanism for this class of scutellarein-*O*-acetamidoalkylbenzylamines derivatives, compound **T-22**, the most potent AChE inhibitor, was selected for further kinetic studies. Graphical analysis of the reciprocal Lineweaver-Burk plots (**Figure 2**) showed both increasing of slopes (decreased V_{max}) and intercepts

(higher K_m) with increasing concentration of the inhibitor. This pattern indicated a mixed-type inhibitory type and revealed that compound **T-22** could bind to both CAS and PAS of AChE.

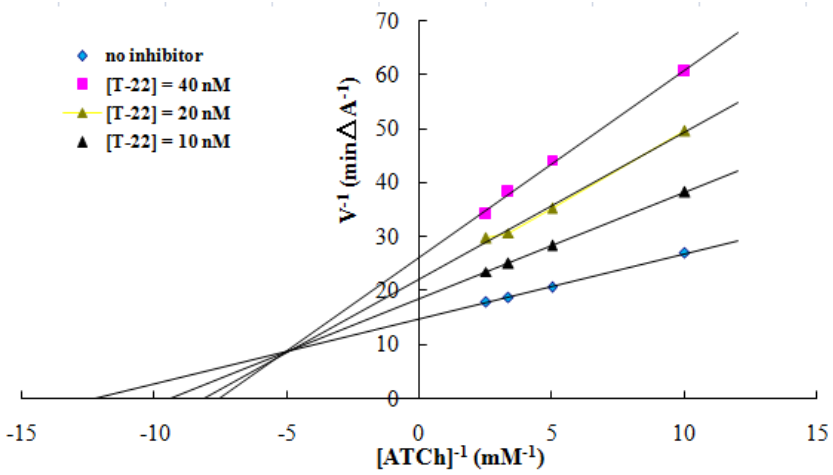

Figure 2. Kinetic study on the mechanism of *Ee*AChE inhibition by compound **T-22**. Merged Lineweaver-Burk reciprocal plots of AChE initial velocity with increasing substrate concentration (100-400 μM) in the absence or presence of **T-22**. Lines were derived from a weighted least-squares analysis of data points.

2.2.3. Molecular modeling study

To further explore the possible interaction mode of the scutellarein-*O*-acetamidoalkylbenzylamines derivatives with *Torpedo californica (Tc)*AChE (PDB code: *1EVE*), a molecular modeling study was performed using the docking program named AUTODOCK 4.2 package with Discovery Studio 2.1 [26]. As shown in **Figure 3**, **T-22** occupied the entire enzymatic catalytic active site (CAS), the mid-gorge sites and the peripheral anionic site (PAS) and could simultaneously bind to both CAS and PAS. In the *Tc*AChE-**T-22** complex, the benzene ring of 4*H*-chromen-4-one was observed to bind to the PAS *via* a π-π interaction with Trp279, and potential hydrophobic interactions with residues Trp279, Leu282, Phe288, Phe331. The 5-hydroxy group at the flavonoid nucleus could bind to the PAS *via* intermolecular hydrogen bond with Ser286. The side chain *N*-(2-methoxybenzyl)ethanamine moiety occupied the CAS of AChE, could bind to the CAS *via* a potential hydrophobic interaction with Ser124, Tyr130, Trp84, Gly123, Ser122, Gly118 and Gly117. The benzene ring at 2-position of 4*H*-chromen-4-one could bind to the mid-gorge sites *via* a π-π interaction with Tyr334, and the amide group could bind to the mid-gorge sites *via* one intermolecular hydrogen bond with Tyr121. In addition, the long chain of methylene,

amide group and the benzene ring at the 2-position of 4*H*-chromen-4-one could fold into a conformation in the gorge that allowed them to interact with Phe330, His440, Ser200 and Gly119 through hydrophobic interaction. Similar to the donepezil complex, water-bridged hydrogen bonding may have occurred under biological circumstances between compound **T-22** and *Tc*AChE. Therefore, the above results provided a reasonable explanation for its highly potent inhibitory activity against AChE.

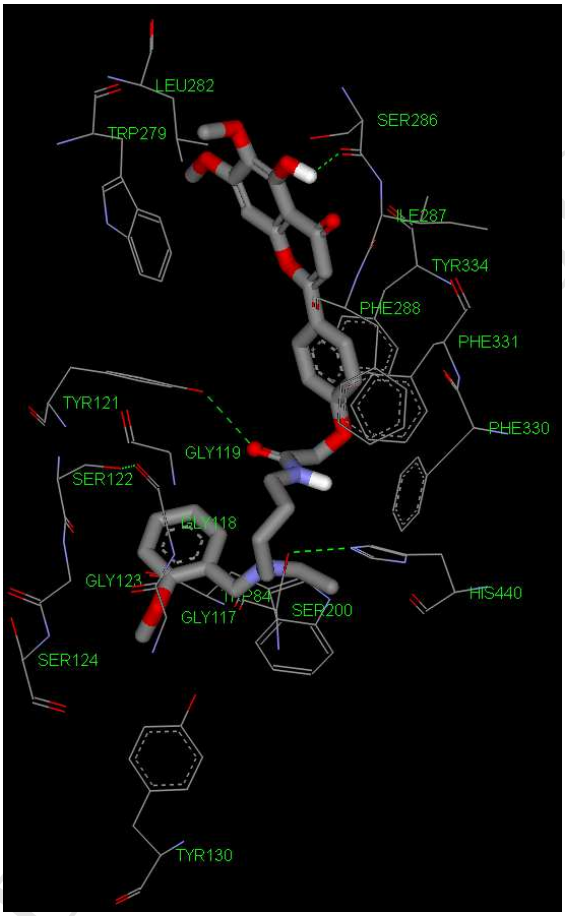

Figure 3. Representative compound **T-22** (colored by atom type) interacting with residues in the binding site of *Tc*AChE (PDB code: *1EVE*), highlighting the protein residues that participate in the main interaction with the inhibitor.

*2.2.4. Metal-chelating properties of compound **T-22***

The ability of compound **T-22** to chelate biometals such as Cu^{2+}, Zn^{2+}, Al^{3+} and Fe^{2+} was studied by UV-visual spectrometry [27]. As shown in **Figure 4**, the UV-vis spectrum of compound **T-22** showed a red shift (the peak at 336 nm shifted to 343 nm) after the addition of $CuCl_2$. The result demonstrated that compound **T-22** could interact with the Cu^{2+} effectively. Similar results were also

obtained when $AlCl_3$ was added, the peak in the UV-vis spectrum of compound **T-22** at 336 nm shift to 357 nm. However, when $ZnCl_2$ and $FeSO_4$ were added, the UV-vis spectrum of **T-22** exhibited no significant shift. The results showed that **T-22** had the selectivity for metal chelation. It was reasonable to estimate that the 5-hydroxyl and 4-carbonyl groups at the flavonoid nucleus contributed to the chelation.

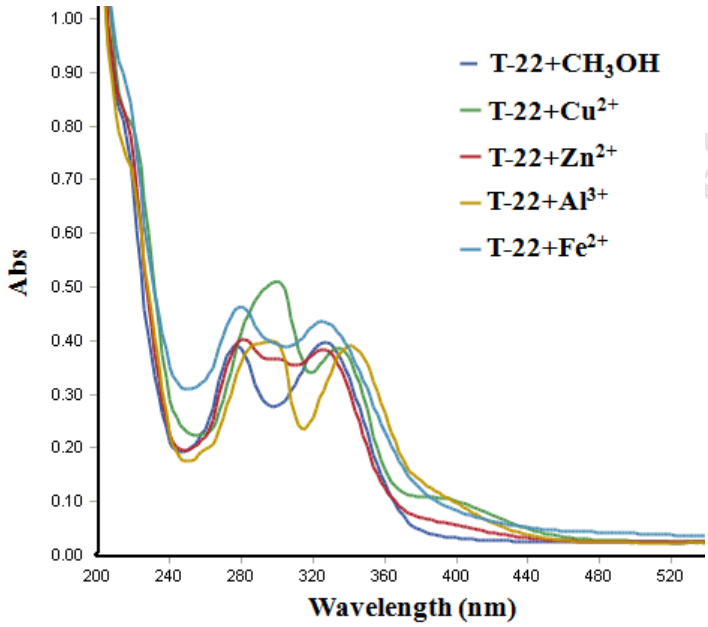

Figure 4. UV spectrum of compound **T-22** (37.5 μM in methanol) alone or in the presence of $CuCl_2$, $ZnCl_2$, $AlCl_3$ and $FeSO_4$ (37.5 μM for all metals in methanol).

The stoichiometry of the **T-22**-Cu^{2+} complex was determined using molar ratio method by preparing solutions of compound **T-22** with increasing amounts of $CuCl_2$. The UV spectra was used to obtain the absorbance of the complex of **T-22** and $CuCl_2$ at different concentrations at 386 nm. According to the **Figure 5**, the absorbance linearly increased at first and then tended to be stable. The two straight lines intersected at a mole fraction of 0.99, indicating a 1:1 stoichiometry of the ligand-Cu^{2+} complex.

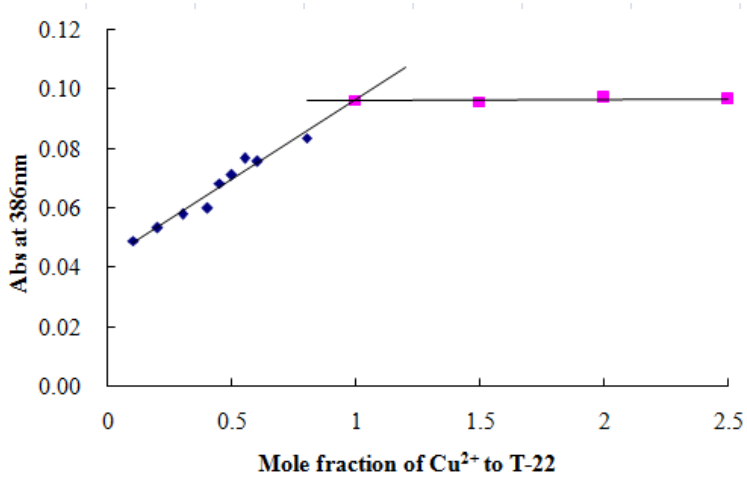

Figure 5. Determination of the stoichiometry of complex-Cu^{2+} by using molar ratio method through titrating the methanol solution of compound **T-22** with ascending amounts of $CuCl_2$. The final concentration of tested compound was 37.5 μM, and the final concentration of Cu^{2+} ranged from 3.75 to 93.75 μM.

2.2.5. Antioxidant activity in vitro.

The antioxidant activities of the target compounds were evaluated by following the ORAC-FL method (Oxygen Radicals Absorbance Capacity by Fluorescence) [28]. Trolox, a vitamin E analogue, was used as a standard, and the results were expressed as Trolox equivalents. The parent compounds **16** and **17** were also tested, which had ORAC-FL values of 1.86 and 3.07 Trolox equivalents, respectively. As shown in **Table 1**, all the compounds exhibited significant antioxidant activities with ORAC-FL values of 0.33-1.18 Trolox equivalents. As expected, introduction of substitutions to 4′-hydroxyl group decreased the radical capture capacity, but the different benzylamines moieties on the side chain had little influence on the radical capture capacity. In general, compounds (**T-17~T-24**) with 5-hydroxyl at the flavonoid nucleus exhibited higher radical capture capacity than that of 5-methoxyl (**T-1~T-16**). It is apparent that the free hydroxyl is crucial to the radical scavenging ability. The compound **T-22** showed good antioxidant activity with an ORAC-FL value of 1.13 trolox equivalents.

2.2.6. Inhibition of self- and HuAChE-induced Aβ aggregation.

The ability of the target compounds to inhibit self-induced $A\beta_{1\text{-}42}$ aggregation was evaluated using the thioflavin T (ThT) fluorescence assay with curcumin as reference compound [29]. Donepezil and the parent compounds (**16** and **17**) were also evaluated for comparative purposes. The results were

summarized in **Table 2**. All the target compounds showed potent inhibitory effect with inhibition ratio ranging from 25.8% to 59.8%. The marketed AD drug, donepezil, did not show any significant inhibitory activity under the same experimental conditions. The parent compounds **16** and **17** also exhibited weak inhibitory potency with inhibition ratio of 6.7% and 9.8%, respectively. It might be possible that the introduction of substitutions improved the inhibitory activity against self-induced A$\beta_{1\text{-}42}$ aggregation. The screening data showed that the 5-hydroxy at flavonoid nucleus (**T-17~T-24**) showed remarkably higher inhibitory activity than that of 5-methoxyl (**T-3**, **T-4**, **T-7**, **T-8**, **T-11**, **T-12**, **T-15** and **T-16**), and different tertiary amine units on the side chain had little influence on the inhibitory activity. The results revealed that the hydrogen bonds are crucial in the interaction between ligand and proteins. The representative compound **T-22** also showed a dose-dependent inhibitory effect on self-induced A$\beta_{1\text{-}42}$ aggregation (43.6% at 12.5 μM, 57.1% at 25 μM, 75.2% at 50 μM).

It was reported that AChE could play a crucial role in accelerating the formation of amyloid fibrils due to the interaction of AChE with Aβ by a hydrophobic environment close to the peripheral anionic site (PAS) [29]. Thus, inhibition of AChE, especially inhibition of PAS of AChE, might affect Aβ aggregation. The kinetic study showed that the representative compound **T-22** exhibited a mix-type inhibition and could bind to both the CAS and PAS of AChE. To further explore the multifunctional properties of these compounds, the better AChE inhibitors, compounds **T-12**, **T-16**, **T-22** and **T-24**, were selected to assess their ability to inhibit the *Hu*AChE-induced A$\beta_{1\text{-}40}$ aggregation by using a thioflavin T fluorescence method. According to the results in **Table 2**, compounds **T-22** and **T-24** (inhibition ratio of 57.3% and 58.1% at 100 μM, respectively) indicated much higher inhibitory potency than donepezil (inhibition ratio of 18.8%), but compounds **T-12** and **T-16** (inhibition ratio of 8.8% and 6.5%, respectively) exhibited lower inhibitory potency than donepezil under the same conditions. Compound **T-22** also showed a dose-dependent inhibitory effect on *Hu*AChE-induced A$\beta_{1\text{-}40}$ aggregation (32.7% at 25 μM, 57.3% at 50 μM, 63.8% at 100 μM). It was apparent that compounds **T-22** and **T-24** with 5-methoxyl group could bond to the PAS of AChE better than donepezil. The results also showed 5-hydroxy at flavonoid nucleus seemed to be beneficial to inhibitory activity against *Hu*AChE-induced A$\beta_{1\text{-}40}$ aggregation, which was consistent with the outcome of inhibitory activity against AChE.

Table 2. Inhibition of self-induced A$\beta_{1\text{-}42}$ aggregation, *Hu*AChE-induced A$\beta_{1\text{-}40}$ aggregation, Cu^{2+}-induced A$\beta_{1\text{-}42}$ aggregation and disaggregation of Cu^{2+}-induced A$\beta_{1\text{-}42}$ aggregation by target

compounds and reference compounds.

Comp.	Inhibition of	% Inhibition of Aβ Aggregation[b,g]			Disaggregation of Aβ
	*Hu*AChE (IC_{50}, μM) [g]	Self-induced[c]	*Hu*AChE -induced[d]	Cu^{2+}-induced[e]	fibrils(%) [f,g]
T-1	NT[h]	44.8 ± 2.4	NT[h]	NT[h]	NT[h]
T-2	NT[h]	37.5 ± 1..0	NT[h]	NT[h]	NT[h]
T-3	NT[h]	29.4 ± 0.8	NT[h]	NT[h]	NT[h]
T-4	NT[h]	26.9 ± 0.6	NT[h]	NT[h]	NT[h]
T-5	NT[h]	34.2 ± 2.2	NT[h]	NT[h]	NT[h]
T-6	NT[h]	25.8 ± 0.4	NT[h]	NT[h]	NT[h]
T-7	NT[h]	27.5 ± 0.6	NT[h]	NT[h]	NT[h]
T-8	NT[h]	42.4 ± 3.2	NT[h]	NT[h]	NT[h]
T-9	NT[h]	29.6 ± 0.9	NT[h]	NT[h]	NT[h]
T-10	NT[h]	29.1 ± 0.4	NT[h]	NT[h]	NT[h]
T-11	NT[h]	41.2 ± 3.9	NT[h]	NT[h]	NT[h]
T-12	0.063 ± 0.005	44.7 ± 1.5	8.8 ± 0.2	NT[h]	NT[h]
T-13	NT[h]	44.3 ± 1.6	NT[h]	NT[h]	NT[h]
T-14	NT[h]	34.4 ± 1.0	NT[h]	NT[h]	NT[h]
T-15	NT[h]	36.1 ± 0.7	NT[h]	NT[h]	NT[h]
T-16	1.25±0.08	35.5 ± 2.1	6.5 ± 0.2	NT[h]	NT[h]
T-17	NT[h]	54.7 ± 1.6	NT[h]	49.3 ± 1.2	57.0 ± 1.0
T-18	NT[h]	59.8 ± 0.9	NT[h]	47.5 ± 1.3	58.9 ± 0.8
T-19	NT[h]	53.9 ± 4.1	NT[h]	44.9 ± 0.7	51.6 ± 1.2
T-20	NT[h]	49.1 ± 2.0	NT[h]	45.1 ± 1.9	54.7 ± 0.6
T-21	NT[h]	56.9 ± 1.0	NT[h]	42.6 ± 0.7	67.1 ± 0.6
T-22	0.039 ± 0.002	57.1 ± 1.9[i]	57.3 ± 0.8[j]	43.4 ± 0.9	66.3 ± 2.6
T-23	NT[h]	53.3 ± 3.1	NT[h]	41.5 ± 0.3	61.2 ± 2.5
T-24	1.37 ± 0.07	56.7 ± 2.7	58.1 ± 1.9	42.7 ± 1.1	65.0 ± 1.3
16	NT[h]	6.7 ± 0.3	NT[h]	NT[h]	NT[h]
17	NT[h]	9.8 ± 0.1	NT[h]	NT[h]	NT[h]

Curcumin	NT[h]	43.1 ± 1.1	NT[h]	58.0 ± 2.1	56.5 ± 2.1
Donepezil	0.012 ± 0.002	<5.0	18.8 ± 1.6	<5.0	NT[h]

[a] From human erythrocytes.

[b] For inhibition of Aβ aggregation, the thioflavin-T fluorescence method was used.

[c] Inhibition of self-induced A$\beta_{1\text{-}42}$ aggregation, the concentration of tested compounds and A$\beta_{1\text{-}42}$ were 25μM.

[d] Inhibition of human AChE-induced A$\beta_{1\text{-}40}$ aggregation. The concentration of tested compounds and A$\beta_{1\text{-}40}$ was 100 and 230 μM, respectively, and the A$\beta_{1\text{-}40}$/HuAChE ratio was equal to 100/1.

[e] Inhibition of Cu^{2+}-induced A$\beta_{1\text{-}42}$ aggregation produced by tested compounds at 25 μM.

[f] Disaggregating Cu^{2+}-induced A$\beta_{1\text{-}42}$ aggregation. The concentration of tested inhibitors and A$\beta_{1\text{-}42}$ were 25 μM.

[g] Data are presented as the mean ± SEM of three independent experiments.

[h] NT=not tested.

[i] Compound **T-22** had a dose-dependent inhibitory effect on self-induced A$\beta_{1\text{-}42}$ aggregation (43.6% at 12.5 μM, 57.1% at 25 μM, 75.2% at 50 μM).

[j] Compound **T-22** had a dose-dependent inhibitory effect on *Hu*AChE-induced A$\beta_{1\text{-}40}$ aggregation (32.7% at 25 μM, 57.3% at 50 μM, 63.8% at 100 μM).

2.2.7. Effects on Cu^{2+}-induced A$\beta_{1\text{-}42}$ aggregation and disaggregation.

In order to investigate the effects on Cu^{2+}-induced A$\beta_{1\text{-}42}$ aggregation, we carried out two individual studies (**Table 2**): inhibitory activity of Cu^{2+}-induced A$\beta_{1\text{-}42}$ aggregation and disaggregation effects on Cu^{2+}-induced A$\beta_{1\text{-}42}$ aggregation by the compounds **T-17~T-24**, using Thioflavin T (ThT) method with curcumin as the reference compound [30]. The A$\beta_{1\text{-}42}$ peptide (25 μM) was first treated with one equivalent of Cu^{2+} for 2 min at room temperature and then incubated with or without the testing compounds for 24 h at 37°C (**Figure 6**). It can be seen that Cu^{2+} could accelerate the aggregation of A$\beta_{1\text{-}42}$. The rate of A$\beta_{1\text{-}42}$ aggregation slowed when adding tested compounds to the samples. It suggested that tested compounds could inhibit Cu^{2+}-induced A$\beta_{1\text{-}42}$ aggregation noticeably by chelating with Cu^{2+}. As shown in **Table 2**, compounds **T-17~T-24** (inhibition ratio ranging 41.5% to 49.3%) exhibited moderate potency compared with curcumin (58.0±2.3%). The results indicated that the inhibitory activity decreased slightly as the length of the side chain carbon spacer increased, for example, **T-17** (49.3%) > **T-19** (44.9%) > **T-21** (42.6%) > **T-23** (41.5%); **T-18** (47.5%) > **T-20** (45.1%) > **T-22** (43.4%) > **T-24** (42.7%), and different

benzylamines units on the side chain had little influence on the inhibitory activity.

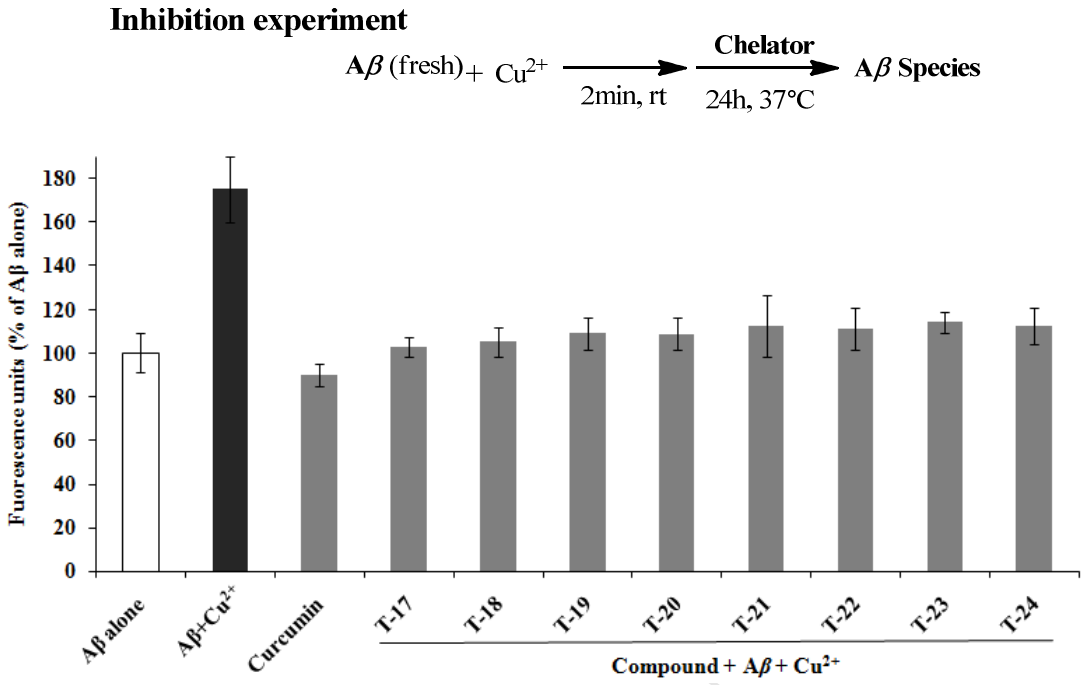

Figure 6. Inhibition of Cu^{2+}-induced aggregation by compounds **T-17~24** and curcumin. The thioflavin-T fluorescence method was used.

For the disaggregation studies, compounds **T-17~T-24** were added to Aβ fibrils, which were generated by reacting A$\beta_{1\text{-}42}$ with one equivalent of Cu^{2+} for 24 h at 37 °C. The results (**Table 2**) showed that all the tested compounds exhibited moderate to good disaggregation potency (disaggregation ratio ranging 51.6% to 67.1%) compared with curcumin (56.5%). The disaggregation potency decreased as the length of the side chain carbon spacer increased, which was consistent with the results of inhibition Cu^{2+}-induced A$\beta_{1\text{-}42}$ aggregation. The compound **T-22** manifested disaggregation potency with inhibition ratio of 66.3% (**Table 2**). Therefore, we can conclude that compound **T-22** is capable of inhibiting Cu^{2+}-induced A$\beta_{1\text{-}42}$ aggregation and disassembling the well-structured Aβ fibrils.

*2.2.8. Cytotoxic effects of compounds **T-12** and **T-22** on SH-SY5Y cells*

To examine the cytotoxicity of the representative compounds **T-12** and **T-22**, human neuronal cell line SH-SY5Y cells were exposed to the tested compounds at three different concentrations (1, 10 and 100 μM) for 24 h, and the cell viability was tested by the 3-(4,5-dimethylthiazol-2-yl)-2,5-diphenyltetrazolium (MTT) assays [22]. As shown in **Figure 7**, **T-12** and **T-22** did not show modified

cell viability up to the concentration of 10 μM. With increased concentration to 100 μM, **T-12** and **T-22** induced a decrease of cell viability (79.4% and 82.4%, respectively), it may be considered that the compound **T-12** with 5-methoxyl at flavonoid nucleus exhibited more cytotoxicity than that of a 5-hydroxyl (**T-22**). These results showed that the target compounds had a wide therapeutic safety range. Further, based on the above results, compounds **T-12** and **T-22** could be selected for further studies to elucidate the neuroprotective mechanisms.

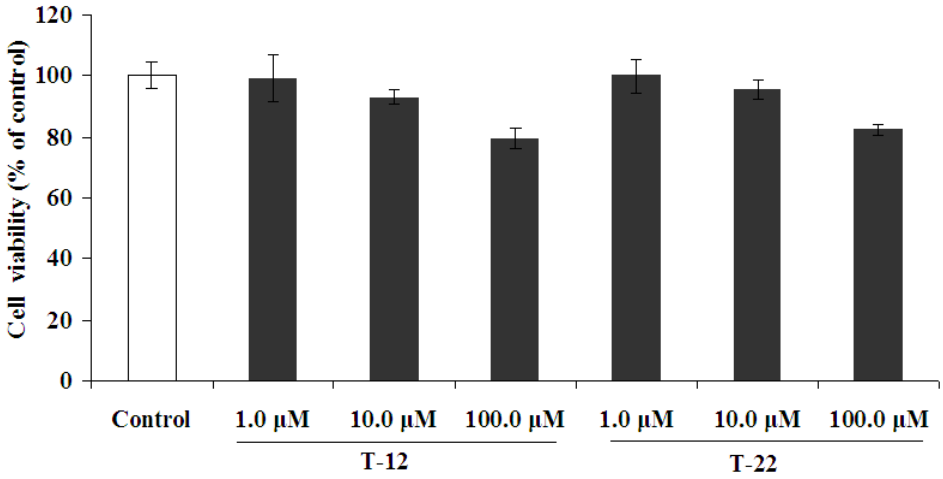

Figure 7. Effects of **T-12** and **T-22** on cell viability in human SH-SY5Y cells. Data are mean values ± SEM of three independent experiments.

2.2.9. Cell protective effects on H_2O_2-induced PC12 cell injury

The neuroprotective capacities of target compounds against oxidative stress were assayed according to the reported protocol [31]. After 100 μM H_2O_2 exposure, cell viability was determined by MTT reduction was markedly decreased to 43.9 % ($p < 0.01$ *vs* control), suggesting high sensitivity to H_2O_2-induced injury. However, compounds **T-12** and **T-22** showed protective effects in a dose-dependent manner against H_2O_2-induced PC12 cell injury (**Figure 8**). At concentrations of 10.0 μM, compounds **T-12** and **T-22** indicated significantly neuroprotective effects and the cell viabilities were 63.3% and 82.7%, respectively. When the concentration is reduced to 1.0 μM, their cell viabilities decreased to 60.1%, and 67.6%, respectively. It revealed that compound **T-22**, with 5-hydroxy on the flavonoid nucleus, had higher cell survival ratio than compound **T-12** with 5-methoxy group. It is reasonable to speculate that the 5-hydroxy can capture the hydroxyl radical, generated by H_2O_2.

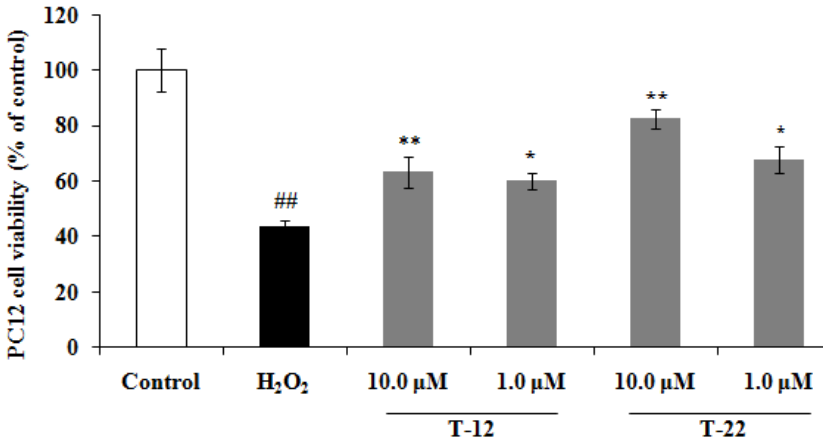

Figure 8. Neuroprotective effect of compound **T-12** and **T-22** at the concentration of 1.0 μM and 10.0 μM on cell injury induced by hydrogen peroxide (H_2O_2, 100 μM) in PC12 cells.

2.2.10. In vivo assay

In vitro the above effects exhibited that compound **T-22** was a promising multifunctional compound for AD treatment. However, the *in vivo* effect of compound **T-22** in models of learning and memory is lacking. In order to further study whether **T-22** could improve memory impairment induced by scopolamine, we carried out the step-down passive avoidance task, which had been used extensively to evaluate potential therapeutic agents for treating AD [22,32]. As shown in **Figure 9**, the step-down latency of mice treated with scopolamine alone (control group) was significantly shorter than that of vehicle-treated mice (normal group, $p < 0.01$). Treatment with compound **T-22** (3.67, 7.33 and 22 mg/kg) increased the latency time in a dose-dependent manner, but the medium dose group (7.33 mg/kg) presented the longest latency time (194.3 sec., $p < 0.01$) of the three dose groups. The medium dose (7.33 mg/kg) of compound **T-22** also showed slightly lower latency time than the drug control group with donepezil (5 mg/kg, 203.7 sec). Meanwhile, the latency time of the high dose of **T-22** (22 mg/kg) demonstrated slightly shorter (176.4 sec) than that of the medium dose. It might be possible that the high dose had some neurotoxicity and the medium dose could be the optimal dose. These results of *in vivo* assay indicated that compound **T-22** could permeate the blood-brain barrier and reverse cognitive deficit by increasing brain cholinergic activity due to the inhibition of AChE.

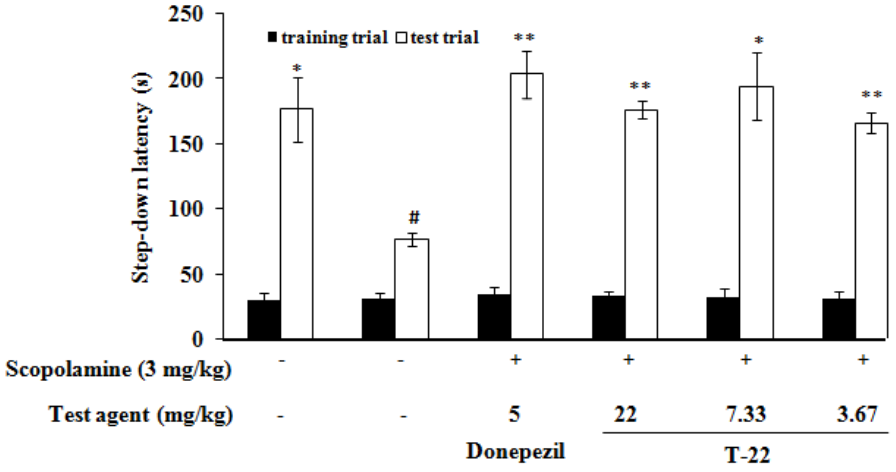

Figure 9. Effects of compound **T-22** on scopolamine-induced memory deficit in the step-down passive avoidance test. Compounds **T-22** (3.67, 7.33 and 22.0 mg/kg, *p.o.*) or donepezil (5.0 mg/kg, *p.o.*) were orally given 1 h before treatment with scopolamine. After 30 min, the mice were treated with scopolamine (3 mg/kg, *i.p.*) and tested in the step-down passive avoidance. Values are expressed as the mean ± SEM (n=10). # $p < 0.05$ *vs* normal group. * $p < 0.05$ and ** $p < 0.01$ *vs* scopolamine-treated control group.

3. Conclusion

In conclusion, to develop effective drugs for the treatment of Alzheimer's disease (AD), a novel series of scutellarein-*O*-acetamidoalkylbenzylamines derivatives **T-1~24** were designed, synthesized and evaluated as multi-targets anti-Alzheimer agents. All of these synthetic compounds showed potent AChE inhibitory activity *in vitro* and high selectivity for AChE over BuChE. Compound **T-22** exhibited the best inhibitory activity toward AChE with IC_{50} value of 0.051 ± 0.003 μM. Moreover, both kinetic analysis of AChE inhibition and the molecular modeling study indicated that compoound **T-22** showed mixed-type inhibition and could bind to both CAS and PAS of AChE. More importantly, Compound **T-22** exhibited good antioxidant potency (1.13*eq* of Trolox), metal chelating properties and significant inhibition of Aβ aggregation. In particular, compound **T-22** inhibited: self-induced A$\beta_{1\text{-}42}$ aggregation, Cu^{2+}-induced A$\beta_{1\text{-}42}$ aggregation and *Hu*AChE-induced A$\beta_{1\text{-}40}$ aggregation by 57.1%, 43.4% and 57.3%, respectively. Furthermore, compound **T-22** could disassemble the well-structured A$\beta_{1\text{-}42}$ fibrils generated Cu^{2+}-induced A$\beta_{1\text{-}42}$ aggregation by 66.3%. Especially, compound **T-22** diaplayed a good neuroprotective effect against H_2O_2-induced PC12 cell injury and a low toxicity in SH-SY5Y cells. More interestingly, the *in vivo* study indicated that mice treated with

T-22 (7.33 mg/kg, *p.o.*) displayed similar step-down latency time compared with the drug control group treated with donepezil (5.0 mg/kg, *p.o.*) in the step-down passive avoidance test. These properties highlight that compound **T-22** may be a promising multifunctional agent for the treatment of AD. Further studies to evaluate compound **T-22** *in vivo* and to develop structural refinements are underway and will be reported in due course.

4. Experiment section

4.1. Chemistry

Unless otherwise noted, all materials were obtained from commercial suppliers and used without further purification. Melting points were recorded on YRT-3 melting-point apparatus (China) and are uncorrected. ^{1}H NMR and ^{13}C NMR spectra were recorded at room temperature in $CDCl_3$ or DMSO-d_6 solutions using a Varian INOVA 400 NMR spectrometer. Chemical shifts are reported in parts per millions (ppm) relative to tetramethylsilane (TMS). Coupling constants are given in hertz, and spin multiplicities are given as s (singlet), brs (broad singlet), d (doublet), t (triplet), or m (multiplet). Mass spectra were recorded on Agilent-6210 TOF LC-MS Spectrometer. The purity of all final compounds was determined by high-performance liquid chromatography (HPLC) analysis to be over 96%. HPLC analysis was carried out on a Shimadzu LC-10Avp plus system with the use of a Kromasil C_{18} column (4.6 mm × 250 mm, 5 μm). All the reactions were monitored by thin-layer chromatography (TLC) on silica gel GF254 plates from Qingdao Haiyang Chemical Co. Ltd. (China), and then visualized with an UV lamp (254 nm). Where appropriate, crude products were purified by column chromatography using silica gel (230-400 mesh) purchased from Qingdao Haiyang Chemical Co. Ltd. (China).

*4.1.1. General procedures for the synthesis of compounds **2a-d**.*

To a suspension of the appropriate dibromoalkane (33 mmol) and potassium carbonate (18 mmol) in anhydrous acetone (30 mL), and potassium phthalimide (15 mmol) was added slowly over a 15 minutes period, and then the reaction mixture was heated under reflux for 8-10 h. The reaction mixture was filtered, and the acetone was evaporated in vacuo. The crude product was purified by column chromatography on silica gel (petroleum/acetone as eluent) to obtain **2a-d** as white solid.

*4.1.1.1. 2-(2-Bromoethyl)-1H-isoindole-1,3(2H)-dione (**2a**).* White solid. Yield 68.1%; mp: 151.3-152.5 °C (lit.[33] 150-153 °C).

*4.1.1.2. 2-(3-Bromopropyl)-1H-isoindoline-1,3(2H)-dione (**2b**).* White solid. Yield 64.7%; mp: 71.0-72.5 °C (lit.[34] 72-75 °C).

*4.1.1.3. 2-(4-Bromobutyl)-1H-isoindoline-1,3(2H)-dione (**2c**).* White solid. Yield 68.3%; mp: 79.1-80.6 °C (lit. [34] 79-81 °C).

*4.1.1.4. 2-(6-Bromohexyl)-1H-isoindoline-1,3(2H)-dione (**2d**).* White solid. Yield 53.7%; mp: 56.8-58.2 °C (lit. [34] 57-58 °C).

*4.1.2. General procedure for the synthesis of compounds **4-7**.*

A mixture of the corresponding secondary amine **3a-d** [23] (5.5 mmol), anhydrous K_2CO_3 (6 mmol) and compounds **2a-d** (5 mmol) were added in CH_3CN (20 ml). The mixture was heated at 65 °C for 8-10 h. The solvent was evaporated under reduced pressure. Then water (25 mL) was added, and the mixture was extracted with dichloromethane (20 mL×3). The combined organic phases were washed with saturated aqueous sodium chloride (30 mL), dried over sodium sulfate, and filtered. The solvent was evaporated under vacuum. The residue was purified on a silica gel chromatography using mixtures of petroleum/acetone as eluent to obtain the oil products **4-7**.

*4.1.2.1. 2-[2-[Methyl(phenylmethyl)amino]ethyl]-1H-isoindole-1,3(2H)-dione (**4a**).* Colorless oil. ^{1}H NMR (400 MHz, $CDCl_3$) δ: 7.84-7.82 (m, 2H), 7.73-7.70 (m, 2H), 7.32-7.30 (m, 2H), 7.15-7.13 (m, 3H), 3.82 (t, *J* = 7.6 Hz, 2H), 3.52 (s, 2H), 2.66 (t, *J* = 7.6 Hz, 2H), 2.30 (s, 3H).

*4.1.2.2. 2-[2-[Ethyl(phenylmethyl)amino]ethyl]-1H-isoindole-1,3(2H)-dione (**4b**).* Colorless oil. ^{1}H NMR (400 MHz, $CDCl_3$) δ: 7.81-7.79 (m, 2H), 7.72-7.69 (m, 2H), 7.17 (d, *J* = 6.8 Hz, 2H), 7.12-7.06 (m, 3H), 3.75 (t, *J* = 6.0 Hz, 2H), 3.57 (s, 2H), 2.70 (t, *J* = 6.0 Hz, 3H), 2.60-2.56 (m, 2H), 1.03 (t, *J* = 6.8 Hz, 3H).

*4.1.2.3.2-[2-[[(2-Methoxyphenyl)methyl]methylamino]ethyl]-1H-isoindole-1,3(2H)-dione(**4c**).*Colorless oil. ^{1}H NMR (400 MHz, $CDCl_3$) δ: 7.83-7.81 (m, 2H), 7.71-7.69 (m, 2H), 7.18-7.13 (m, 2H), 6.78 (d, *J* = 6.4 Hz, 1H), 6.74 (t, *J* = 7.2 Hz, 1H), 3.85 (t, *J* = 6.4 Hz, 2H), 3.73 (s, 3H), 3.59 (s, 2H), 2.71 (t, *J* = 7.2 Hz, 2H), 2.33 (s, 3H).

*4.1.2.4.2-[2-[[(2-Methoxyphenyl)methyl]ethylamino]ethyl]-1H-isoindole-1,3(2H)-dione(**4d**).*Colorless oil. ^{1}H NMR (400 MHz, $CDCl_3$) δ 7.79-7.78 (m, 2H), 7.69-7.68 (m, 2H), 7.19 (d, *J* = 7.2 Hz, 1H), 7.09 (t, *J* = 7.2 Hz, 1H), 6.73 (t, *J* = 7.6 Hz, 1H), 6.67 (t, *J* = 7.2 Hz, 1H), 3.77 (t, *J* = 6.4 Hz, 2H), 3.73 (s, 3H), 3.63 (s, 2H), 2.74 (t, *J* = 6.0 Hz, 2H), 2.64-2.61 (m, 2H), 1.05 (t, *J* = 6.8 Hz, 3H).

*4.1.2.5. 2-[3-[Methyl(phenylmethyl)amino]propyl]-1H-isoindole-1,3(2H)-dione (**5a**),* colorless oil.

^{1}H NMR (400 MHz, $CDCl_3$) 7.84-7.82 (m, 2H), 7.72-7.69 (m, 2H), 7.29-7.23 (m, 5H), 3.76 (t, *J* = 7.2 Hz, 2H), 3.48 (s, 2H), 2.45 (t, *J* =7.2 Hz, 2H), 2.17 (s, 3H), 1.92-1.87 (m, 2H).

*4.1.2.6. 2-[3-[Ethyl(phenylmethyl)amino]propyl]-1H-isoindole-1,3(2H)-dione (**5b**).*Colorless oil. ^{1}H NMR (400 MHz, $CDCl_3$) δ: 7.84-7.80 (m, 2H), 7.73-7.70 (m, 2H), 7.32 (d, *J* = 6.8 Hz, 2H), 7.27 (t, *J* = 6.8 Hz, 2H), 7.19 (t, *J* = 6.8 Hz, 1H), 3.72 (t, *J* = 7.2 Hz, 2H), 3.55 (s, 2H), 2.54-2.48 (m, 4H), 1.88-1.82 (m, 2H), 1.02 (t, *J* = 7.2 Hz, 3H).

*4.1.2.7.2-[3-[[(2-Methoxyphenyl)methyl]methylamino]propyl]-1H-isoindole-1,3(2H)-dione(**5c**).*Colo rless oil. ^{1}H NMR (400 MHz, $CDCl_3$) δ 7.85-7.83 (m, 2H), 7.73-7.71 (m, 2H), 7.30 (d, *J* = 7.2 Hz, 1H), 7.20 (t, *J* = 7.2 Hz, 1H), 6.88 (t, *J* = 7.2 Hz, 1H), 6.84 (d, *J* = 7.2 Hz, 1H), 3.82 (s, 3H), 3.77 (t, *J* = 7.2 Hz, 2H), 3.51 (s, 2H), 2.50 (t, *J* = 7.2 Hz, 2H), 2.21 (s, 3H), 1.95-1.92 (m, 2H).

*4.1.2.8. 2-[3-[[(2-Methoxyphenyl)methyl]ethylamino]propyl]-1H-isoindole-1,3(2H)-dione (**5d**).* Colorless oil. ^{1}H NMR (400 MHz, $CDCl_3$) δ 7.84-7.82 (m, 2H), 7.72-7.69 (m, 2H), 7.43 (d, *J* = 7.2 Hz, 1H), 7.20 (t, *J* = 7.2 Hz, 1H), 6.90 (t, *J* = 7.2 Hz, 1H), 6.83 (d, *J* = 7.2 Hz, 1H), 3.82 (s, 3H), 3.72 (t, *J* = 6.8 Hz, 2H), 3.70 (s, 2H), 2.65-2.57 (m, 4H), 1.96-1.91 (m, 2H), 1.11 (t, *J* = 7.2 Hz, 3H).

*4.1.2.8. 2-[4-[Methyl(phenylmethyl)amino]butyl]-1H-isoindole-1,3(2H)-dione (**6a**).*Colorless oil. ^{1}H NMR (400 MHz, $CDCl_3$) δ 7.85-7.83 (m, 2H), 7.71-7.70 (m, 2H), 7.29-7.22 (m, 5H), 3.69 (t, *J* = 7.2 Hz, 2H), 3.51 (s, 2H), 2.43 (t, *J* = 6.8 Hz, 2H), 2.19 (s, 3H), 1.72-1.68 (m, 2H), 1.60-1.56 (m, 2H).

*4.1.2.9. 2-[4-[Ethyl(phenylmethyl)amino]butyl]-1H-isoindole-1,3(2H)-dione (**6b**).*Colorless oil. ^{1}H NMR (400 MHz, $CDCl_3$) δ 7.85-7.83 (m, 2H), 7.73-7.71 (m, 2H), 7.33 (d, *J* = 6.8 Hz, 2H), 7.29 (t, *J* = 6.8 Hz, 2H), 7.22 (t, *J* = 6.8 Hz, 1H), 3.67 (t, *J* = 7.2 Hz, 2H), 3.58 (s, 2H), 2.57-2.46 (m, 4H), 1.71-1.66 (m, 2H), 1.56-1.52 (m, 2H), 1.02 (t, *J* = 7.2 Hz, 3H).

*4.1.2.10. 2-[4-[[(2-Methoxyphenyl)methyl]methylamino]butyl]-1H-isoindole-1,3(2H)-dione (**6c**).* Colorless oil. ^{1}H NMR (400 MHz, $CDCl_3$) δ 7.85-7.83 (m, 2H), 7.73-7.71 (m, 2H), 7.30 (d, *J* = 7.2 Hz, 1H), 7.21 (t, *J* = 7.2 Hz, 1H), 6.91 (t, *J* = 7.2 Hz, 1H), 6.85 (d, *J* = 7.2 Hz, 1H), 3.81 (s, 3H), 3.71 (t, *J* = 6.8 Hz, 2H), 3.49 (s, 2H), 2.44 (t, *J* = 7.2 Hz, 2H), 2.20 (s, 3H), 1.74-1.69 (m, 2H), 1.62-1.59 (m, 2H).

*4.1.2.11. 2-[4-[[(2-Methoxyphenyl)methyl]ethylamino]butyl]-1H-isoindole-1,3(2H)-dione (**6d**).* Colorless oil. ^{1}H NMR (400 MHz, $CDCl_3$) δ 7.84-7.81 (m, 2H), 7.72-7.69 (m, 2H), 7.39 (d, *J* = 7.2 Hz, 1H), 7.19 (t, *J* = 7.2 Hz, 1H), 6.91 (t, *J* = 7.2 Hz, 1H), 6.83 (d, *J* = 7.2 Hz, 1H), 3.81 (s, 3H), 3.68 (t, *J* = 6.8 Hz, 2H), 3.57 (s, 2H), 2.53-2.47 (m, 4H), 1.73-1.66 (m, 2H), 1.56-1.51 (m, 2H), 1.04 (t, *J*

= 7.2 Hz, 3H).

*4.1.2.12. 2-[6-[Methyl(phenylmethyl)amino]hexyl]-1H-isoindole-1,3(2H)-dione (**7a**).* Colorless oil. ^{1}H NMR (400 MHz, $CDCl_3$) δ 7.85-7.82 (m, 2H), 7.73-7.70 (m, 2H), 7.29-7.23 (m, 5H), 3.67 (t, *J* = 7.2 Hz, 2H), 3.48 (s, 2H), 2.36 (q, *J* = 7.2 Hz, 2H), 2.18 (s, 3H), 1.69-1.66 (m, 2H), 1.55-1.49 (m, 2H), 1.38-1.31 (m, 4H).

*4.1.2.13. 2-[6-[Ethyl(phenylmethyl)amino]hexyl]-1H-isoindole-1,3(2H)-dione (**7b**).* Colorless oil. ^{1}H NMR (400 MHz, $CDCl_3$) δ 7.85-7.82 (m, 2H), 7.73-7.71 (m, 2H), 7.36 (d, *J* = 7.2 Hz, 2H), 7.31 (t, *J* = 7.2 Hz, 2H), 7.24 (t, *J* = 6.8 Hz, 1H), 3.66 (t, *J* = 7.2 Hz, 2H), 3.63 (s, 2H), 2.56 (q, *J* = 7.2 Hz, 2H), 2.47 (t, *J* = 7.2 Hz, 2H), 1.67-1.65 (m, 2H), 1.56-1.49 (m, 2H), 1.33-1.29 (m, 4H), 1.07 (t, *J* = 7.2 Hz, 3H).

*4.1.2.14. 2-[6-[[(2-Methoxyphenyl)methyl]methylamino]hexyl]-1H-isoindole-1,3(2H)-dione (**7c**).* Colorless oil. ^{1}H NMR (400 MHz, $CDCl_3$) δ 7.85-7.83 (m, 2H), 7.72-7.70 (m, 2H), 7.30 (d, *J* = 7.2 Hz, 1H), 7.22 (t, *J* = 7.2 Hz, 1H), 6.92 (t, *J* = 7.2 Hz, 1H), 6.85 (d, *J* = 7.2 Hz, 1H), 3.82 (s, 3H), 3.68 (t, *J* = 7.2 Hz, 2H), 3.49 (s, 2H), 2.38 (q, *J* = 7.2 Hz, 2H), 2.20 (s, 3H), 1.70-1.65 (m, 2H), 1.55-1.51 (m, 2H), 1.39-1.35 (m, 4H).

*4.1.2.15. 2-[4-[[(2-Methoxyphenyl)methyl]ethylamino]butyl]-1H-isoindole-1,3(2H)-dione (**7d**).* Colorless oil. ^{1}H NMR (400 MHz, $CDCl_3$) δ 7.85-7.83 (m, 2H), 7.72-7.70 (m, 2H), 7.40 (d, *J* = 8.0 Hz, 1H), 7.20 (t, *J* = 8.0 Hz, 1H), 6.92 (t, *J* = 8.0 Hz, 1H), 6.84 (d, *J* = 8.0 Hz, 1H), 3.81 (s, 3H), 3.66 (t, *J* = 7.2 Hz, 2H), 3.58 (s, 2H), 2.52 (q, *J* = 6.8 Hz, 2H), 2.44 (t, *J* = 6.4 Hz, 2H), 1.68-1.65 (m, 2H), 1.50-1.47 (m, 2H), 1.33-1.31 (m, 4H), 1.04 (t, *J* = 6.8 Hz, 3H).

*4.1.3. General procedure for the synthesis of compounds **8-11**.*

Compounds **4-7** (10 mmol) and 80% hydrazine hydrate solution (30 mmol) were added in ethanol (50 mL). The reaction mixture was heated under reflux for 3-5 h, and then filtered, the filtrate was concentrated under reduced pressure. The residue was dissolved in dichloromethane (50 mL), washed with water (30 mL×2) and saturated aqueous sodium chloride (30 mL), dried over Na_2SO_4, and filtered. The solvent was evaporated under reduced pressure to obtain compounds **8-11** as light yellow oil with high purity. The products were dried over P_2O_5 under vacuum for 24 h and used for further reactions directly.

*4.1.3.1. (E)-1-(6-hydroxy-2,3,4-trimethoxyphenyl)-3-(4-(methoxymethoxy)phenyl)prop-2-en-1-one (**14**).* To a solution of *p*-hydroxybenzaldehyde (10 mmol) and potassium carbonate (11 mmol) in 15

mL anhydrous acetone, chloromethyl methy ether (10.5 mmol) was added slowly. The mixture was heated at reflux for 5-6 h, cooled to room temperature and filtered, the filtered was concentrated under reduced pressure to give compound **13** as light yellow oil, which was used in the next step without further purification.

To a mixture of the start material 6-hydroxy-2,3,4-trimethoxyacetophenone **12** (5 mmol) with the 4-(methoxymethoxy)benzaldehyde **13** (5.5 mmol) in EtOH (7 mL). An amount of 30% aqueous KOH (6 mmol) solution was slowly added to the reaction. The mixture was stirred for 3-4 days at room temperature, and then poured into ice-cold water. The mixture was acidified with 10% HCl and stirred at romm temperature for overnight. The yellow solid formed was collected by filtration and recrystallized from 80% ethanol to give compound **14**. Yield 90%; mp: 94.2-94.5°C; ^{1}H NMR (400 MHz, $CDCl_3$) δ 13.78 (s, 1H), 7.87 (d, *J* = 15.6 Hz, 1H), 7.81 (d, *J* = 15.6 Hz, 1H), 7.60 (d, *J* = 8.8 Hz, 2H), 7.08 (d, *J* = 8.8 Hz, 2H), 6.30 (s, 1H), 5.23 (s, 2H), 3.93 (s, 3H), 3.91 (s, 3H), 3.84 (s, 3H), 3.50 (s, 3H).

*4.1.3.2. 4,2'-Dihytroxy-4',5',6'-trimethoxychalcone (**15**).* A mixture of compound **14** (10 mmol) and 10%HCl (6 mL) in 8 mL ethanol was heated at 50 °C for 3 h, then cooled to room temperature and poured into ice-water. The mixture was stirred at room temperature for overnight. The yellow solid formed was collected by filtration and recrystallized from 90% ethanol to give compound **15** as yellow solid. Yield 91%; mp: 146.2-147.2°C; ^{1}H NMR (400 MHz, $CDCl_3$) δ 13.79 (s, 1H), 7.86 (d, *J* = 16.0 Hz, 1H), 7.81 (d, *J* = 16.0 Hz, 1H), 7.54 (d, *J* = 8.4 Hz, 2H), 6.88 (d, *J* = 8.4 Hz, 2H), 6.30 (s, 1H), 5.41 (brs, 1H), 3.93 (s, 3H), 3.90 (s, 3H), 3.84 (s, 3H).

*4.1.3.3. 4'-Hydroxy-5,6,7-trimethoxyflavone (**16**).* Compound **15** (5 mmol) and potassium iodide (0.2 mmol) was added to a solution of *conc.* H_2SO_4 (0.1 mL) in 10 mL DMSO. The mixture was heated at 100°C for 3-5 h, then poured into ice-water containing sodium thiosulfate (0.21 mmol) and stirred at room temperature for overnight. The solid formed was collected by filtration and recrystallized from 80% alcohol to afford yellow solid **16**. Yield 91.6%; mp: 224.1-225.4°C; ^{1}H NMR (400 MHz, DMSO-d_6) δ 10.25 (s, 1H), 7.91 (d, *J* = 8.4 Hz, 2H), 7.19 (s, 1H), 6.92 (d, *J* = 8.8 Hz, 2H), 6.64 (s, 1H), 3.95 (s, 3H), 3.80 (s, 3H), 3.77 (s, 3H).

*4.1.3.4. 5,4'-Dihydroxy-6,7-dimethoxyflavone (**17**).* To a solution of compound **16** (5 mmol) in 15 mL anhydrous acetonitrile was added aluminium chloride (10 mmol). The mixture was heat at 60 °C for 1 h, then added 10 mL10% HCl, and refluxed for 1 h. The solution was poured into ice-water,

filtrating, the residue was recrystallized from methoxyethanol to afford light yellow compounds **17**. Yield 90.1%; mp: 261.1-262.3°C; ^{1}H NMR (400 MHz, DMSO-d_6) δ 12.94 (s, 1H), 10.41 (s, 1H), 7.98 (d, J = 9.2 Hz, 2H), 6.95-6.93 (m, 3H), 6.87 (s, 1H), 3.93 (s, 3H), 3.74 (s, 3H).

*4.1.4. General procedure for the synthesis of compounds **18a-b**.*

To a solution of compounds **16** or **17** (5 mmol) and anhydrous K_2CO_3 (6.0 mmol) in CH_3CN, and ethyl bromoacetate (5.5 mmol) was slowly added. The reaction mixture was heated at 65 °C and stirred for 8-10 h under an argon atmosphere. After complete reaction, the solvent was evaporated under reduced pressure. Then water (50 mL) was added to the residue and the mixture was extracted with dichloromethane (30 mL×3). The combined organic phases were washed with saturated Na_2CO_3 aqueous solution (30 mL×3) and saturated aqueous sodium chloride (60 mL), dried over Na_2SO_4, and filtered. The solvent was evaporated to dryness. The residue was purified on a silica gel chromatography using mixtures of petroleum/acetone as eluent to obtain the compound **18a-b** as light yellow solid.

*4.1.4.1. Ethyl 2-(4-(5,6,7-trimethoxy-4-oxo-4H-chromen-2-yl)phenoxy)acetate (**18a**).* Light yellow solid. Yield 89.5%; mp: 132.2-133.6°C; ^{1}H NMR (400 MHz, $CDCl_3$) δ 7.84 (d, 2H, J = 8.4 Hz), 7.02 (d, 2H, J = 8.8 Hz), 6.80 (s, 1H), 6.64 (d, J = 5.2 Hz, 1H), 4.70 (s, 2H), 4.30 (q, J_1 = 14.0 Hz, J_2 = 7.2 Hz, 2H), 3.99 (s, 6H), 3.92 (s, 3H), 1.32 (t, J = 7.2 Hz, 3H).

*4.1.4.2. Ethyl 2-(4-(5-hydroxy-6,7-dimethoxy-4-oxo-4H-chromen-2-yl)phenoxy)acetate (**18b**).* Light yellow solid. Yield 80.7%; mp: 157.2-158.1°C; ^{1}H NMR (400 MHz, $CDCl_3$) δ 12.68 (brs, 1H), 7.86 (d, J = 9.2 Hz, 2H), 7.03 (d, J = 8.8 Hz, 2H), 6.59 (s, 1H), 6.55 (s, 1H), 4.72 (s, 2H), 4.30 (q, J = 7.2 Hz, 2H), 3.97 (s, 3H), 3.93 (s, 3H), 1.32 (t, J = 6.8 Hz, 3H).

*4.1.5. General procedure for the synthesis of compounds **19a-b**.*

The mixture of LiOH (15 mmol) in water (15 mL) was added to a solution of compounds **18a-b** in THF (20 mL), and then heated under reflux for 2 h. The solution was concentrated in vacuo, diluted with water (20 mL), acidified with 10% HCl. The solid formed was collected by filtration, washed with water, dried, and recrystallized from ethanol to afford light yellow compounds **19a-b**.

*4.1.5.1. 2-(4-(5,6,7-Trimethoxy-4-oxo-4H-chromen-2-yl)phenoxy)acetic acid (**19a**).* Light yellow solid. Yield 83.2%; mp: 234.0-235.7°C; ^{1}H NMR (400 MHz, DMSO-d_6) δ 13.15 (s, 1H), 8.02 (d, 2H, J = 8.8 Hz), 7.23 (s, 1H), 7.09 (d, 2H, J = 9.2 Hz), 6.73 (s, 1H), 4.82 (s, 2H), 3.95 (s, 3H), 3.80 (s, 3H), 3.77 (s, 3H).

*4.1.5.2. 2-(4-(5-Hydroxy-6,7-dimethoxy-4-oxo-4H-chromen-2-yl)phenoxy)acetic acid (**19b**).*Light yellow solid. Yield 88.7%; mp: 228.3-229.7°C; ^{1}H NMR (400 MHz, DMSO-d_6) δ 13.18 (s, 1H), 12.88 (s, 1H), 8.07 (d, 2H, *J* = 8.8 Hz), 7.12 (d, 2H, *J* = 8.8 Hz), 6.97 (s, 1H), 6.96 (s, 1H), 4.84 (s, 2H), 3.93 (s, 3H), 3.74 (s, 3H).

*4.1.6. General procedure for the synthesis of compounds **T-1~T-24**.*

To a mixture of (1-(3-dimethylaminopropyl)-3-ethylcarbodiimide hydrochloride (EDCI, 0.45 mmol) and compounds **19a-b** (0.3 mmol) in THF (3 mL) was stirred for 0.5 h at room temperature, then added the solution of the appropriate intermediates **8-11** (0.33 mmol) in THF (1 mL). And then was stirred at room temperature for overnight. The solvent was evaporated in vacuo. The residue was dissolved in dichloromethane (30 mL), washed with water (20 mL×2) and saturated aqueous sodium chloride (30 mL), dried over sodium sulfate, and filtered. The solvent was evaporated under a vacuum to give the crude product which was purified by column chromatography on silica gel (CH_2Cl_2/CH_3OH as eluent) to obtain the desired products **T1-24**.

*4.1.6.1.N-(2-(benzyl(methyl)amino)ethyl)-2-(4-(5,6,7-trimethoxy-4-oxo-4H-chromen-2-yl)phenoxy)acetamide (**T-1**).* Light yellow oil. Yield 41.3%; Purity: 98.2% (by HPLC); ^{1}H NMR (400 MHz, $CDCl_3$) δ 7.88 (d, 2H, *J* = 8.8 Hz), 7.29-7.24 (m, 5H), 7.19 (brs, 1H), 7.09 (d, *J* = 8.4 Hz), 6.81 (s, 1H), 6.61 (s, 1H), 4.55 (s, 2H), 3.99 (s, 6H), 3.93 (s, 3H), 3.54 (s, 2H), 3.48-3.44 (m, 2H), 2.59-2.57 (m, 2H), 2.24 (s, 3H); ^{13}C NMR (100 MHz, $CDCl_3$) δ 177.1, 167.2, 160.5, 159.5, 157.6, 154.4, 152.5, 140.3, 138.6, 128.7 (2C), 128.3 (2C), 127.8 (2C), 127.2, 125.2, 115.0 (2C), 112.7, 107.4, 96.2, 67.3, 62.2, 62.1, 61.5, 56.2, 55.0, 41.6, 36.1; MS (ESI) m/z 533.3 $[M + H]^+$.

*4.1.6.2.N-(2-(benzyl(ethyl)amino)ethyl)-2-(4-(5,6,7-trimethoxy-4-oxo-4H-chromen-2-yl)phenoxy)acetamide (**T-2**).* Light yellow oil. Yield 49.5%; Purity: 98.8% (by HPLC); ^{1}H NMR (400 MHz, $CDCl_3$) δ 7.88 (d, 2H, *J* = 8.8 Hz), 7.29-7.23 (m, 5H), 7.21 (brs, 1H), 7.07 (d, *J* = 8.0 Hz), 6.81 (s, 1H), 6.61 (s, 1H), 4.53 (s, 2H), 3.99 (s, 6H), 3.93 (s, 3H), 3.59 (s, 2H), 3.41-3.38 (m, 2H), 2.65-2.52 (m, 4H), 1.03 (t, *J* = 7.2 Hz, 3H); ^{13}C NMR (100 MHz, $CDCl_3$) δ 177.0, 167.0, 160.5, 159.5, 157.6, 154.3, 152.4, 140.2, 139.1, 128.5 (2C), 128.2 (2C), 127.8 (2C), 126.9, 125.1 114.9 (2C), 112.7, 107.3, 96.1, 67.2, 62.0, 61.4, 57.7, 56.2, 51.3, 47.0, 36.1, 11.7; MS (ESI) m/z 347.3 $[M + H]^+$.

*4.1.6.3.N-(2-((2-methoxybenzyl)(methyl)amino)ethyl)-2-(4-(5,6,7-trimethoxy-4-oxo-4H-chromen-2-yl)phenoxy)acetamide (**T-3**).* Light yellow oil. Yield 41.6%; Purity: 97.6% (by HPLC); ^{1}H NMR (400 MHz, $CDCl_3$) δ 7.83 (d, *J* = 8.4 Hz, 2H), 7.47 (brs, 1H), 7.32 (d, *J* = 7.2 Hz, 1H), 7.27 (t, *J* = 6.8 Hz,

1H), 7.04 (d, *J* = 8.8 Hz, 2H), 6.92-6.87 (m, 2H), 6.80 (s, 1H), 6.59 (s, 1H), 4.55 (s, 2H), 3.99 (s, 6H), 3.92 (s, 3H), 3.81 (s, 3H), 3.62 (s, 2H), 3.52-3.50 (m, 2H), 2.66-2.65 (m, 2H), 2.27 (s, 3H); ^{13}C NMR (100 MHz, $CDCl_3$) δ 177.0, 167.3, 160.6, 159.6, 157.7, 157.6, 154.3, 152.4, 140.2, 130.5, 128.6, 127.7 (2C), 125.2, 125.0, 120.3, 115.1 (2C), 112.7, 110.4, 107.3, 96.2, 67.3, 62.1, 61.4, 56.2, 55.5, 55.3, 54.9, 41.8, 36.0; MS (ESI) m/z 563.2 $[M + H]^+$.

*4.1.6.4.N-(2-(ethyl(2-methoxybenzyl)amino)ethyl)-2-(4-(5,6,7-trimethoxy-4-oxo-4H-chromen-2-yl)phenoxy)acetamide (**T-4**).* Light yellow oil. Yield 39.5%; Purity: 97.3% (by HPLC); ^{1}H NMR (400 MHz, $CDCl_3$) δ 7.87 (d, *J* = 8.8 Hz, 2H), 7.40 (brs, 1H), 7.33 (d, *J* = 7.2 Hz, 1H), 7.26 (t, *J* = 7.2 Hz, 1H), 7.04 (d, *J* = 8.0 Hz, 2H), 6.92-6.87 (m, 2H), 6.83 (s, 1H), 6.62 (s, 1H), 4.56 (s, 2H), 4.01 (s, 6H), 3.95 (s, 3H), 3.82 (s, 3H), 3.63 (s, 2H), 3.47-3.43 (m, 2H), 2.66 (t, *J* = 7.2 Hz, 2H), 2.56-2.50 (m, 2H), 1.00 (t, *J* = 7.2 Hz, 3H); ^{13}C NMR (100 MHz, $CDCl_3$) δ 177.1, 167.0, 160.6, 159.6, 157.6, 157.6, 154.3, 152.4, 140.2, 130.0, 128.1, 127.7 (2C), 125.0, 120.2, 114.9 (2C), 112.7, 110.3, 107.3, 96.1, 67.2, 62.1, 61.4, 56.2, 55.2, 51.5, 51.2, 47.4, 36.2, 11.7; MS (ESI) m/z 577.4 $[M + H]^+$.

*4.1.6.5.N-(3-(benzyl(methyl)amino)propyl)-2-(4-(5,6,7-trimethoxy-4-oxo-4H-chromen-2-yl)phenoxy)acetamide (**T-5**).* Light yellow oil. Yield 51.1%; Purity: 97.9% (by HPLC); ^{1}H NMR (400 MHz, $CDCl_3$) δ 8.07 (brs, 1H), 7.80 (d, *J* = 8.4 Hz, 2H), 7.31-7.24 (m, 5H), 6.88 (d, *J* = 8.8 Hz, 2H), 6.79 (s, 1H), 6.58 (s, 1H), 4.55 (s, 2H), 3.99 (s, 6H), 3.92 (s, 3H), 3.51 (s, 2H), 3.47-3.42 (m, 2H), 2.52-2.49 (m, 2H), 2.17 (s, 3H), 1.75-1.72 (m, 2H); ^{13}C NMR (100 MHz, $CDCl_3$) δ 176.9, 167.1, 160.5, 159.5, 157.5, 154.2, 152.3, 140.1, 138.1, 129.0 (2C), 128.2 (2C), 127.6 (2C), 127.1, 124.8, 114.8 (2C), 112.6, 107.1, 96.1, 67.2, 62.9, 62.0, 61.4, 56.1 (2C), 41.6, 38.9, 25.4; MS (ESI) m/z 547.3 $[M + H]^+$.

*4.1.6.6.N-(3-(benzyl(ethyl)amino)propyl)-2-(4-(5,6,7-trimethoxy-4-oxo-4H-chromen-2-yl)phenoxy)acetamide (**T-6**).* Light yellow oil. Yield 53.3%; Purity: 98.6% (by HPLC); ^{1}H NMR (400 MHz, $CDCl_3$) δ 7.90 (brs, 1H), 7.82 (d, *J* = 8.8 Hz, 2H), 7.31-7.20 (m, 5H), 6.92 (d, *J* = 8.4 Hz, 2H), 6.80 (s, 1H), 6.59 (s, 1H), 4.54 (s, 2H), 3.99 (s, 3H), 3.98 (s, 3H), 3.92 (s, 3H), 3.56 (s, 2H), 3.44-3.37 (m, 2H), 2.55-2.52 (m, 4H), 1.73-1.71 (m, 2H), 1.07 (t, *J* = 7.2 Hz, 3H); ^{13}C NMR (100 MHz, $CDCl_3$) δ 177.1, 167.2, 160.6, 159.5, 157.6, 154.4, 152.4, 140.3, 138.7, 129.0 (2C), 128.2 (2C), 127.7 (2C), 127.0, 125.0, 114.9 (2C), 112.7, 107.3, 96.1, 67.3, 62.1, 61.5, 58.4, 56.2, 51.8, 47.1, 39.0, 25.5, 11.1; MS (ESI) m/z 561.3 $[M + H]^+$.

4.1.6.7.N-(3-((2-methoxybenzyl)(methyl)amino)propyl)-2-(4-(5,6,7-trimethoxy-4-oxo-4H-chromen-2-

*yl)phenoxy)acetamide (**T-7**).* Light yellow oil. Yield 51.1%; Purity: 98.3% (by HPLC); ^{1}H NMR (400 MHz, $CDCl_3$) δ 8.41 (brs, 1H), 7.74 (d, *J* = 8.8 Hz, 2H), 7.25-7.22 (m, 2H), 6.92 (t, *J* = 7.2 Hz, 2H), 6.85 (d, *J* = 8.4 Hz, 2H), 6.79 (s, 1H), 6.56 (s, 1H), 4.51 (s, 2H), 3.99 (s, 6H), 3.92 (s, 3H), 3.79 (s, 3H), 3.52 (s, 2H), 3.49-3.43 (m, 2H), 2.57-2.53 (m, 2H), 2.09 (s, 3H), 1.75-1.73 (m, 2H); ^{13}C NMR (100 MHz, $CDCl_3$) δ 177.0, 167.1, 160.6, 159.6, 157.9, 157.5, 154.3, 152.3, 140.2, 131.1, 128.6, 127.5 (2C), 126.0, 124.6, 120.0, 114.7 (2C), 112.6, 110.3, 107.1, 96.1, 67.1, 62.0, 61.4, 57.0, 56.8, 56.2, 54.9, 41.4, 39.5, 25.2; MS (ESI) m/z 577.4 $[M + H]^+$.

*4.1.6.8.N-(3-(ethyl(2-methoxybenzyl)amino)propyl)-2-(4-(5,6,7-trimethoxy-4-oxo-4H-chromen-2-yl)phenoxy)acetamide (**T-8**).* Light yellow oil. Yield 37.6%; Purity: 98.2% (by HPLC); ^{1}H NMR (400 MHz, $CDCl_3$) δ 8.15 (brs, 1H), 7.79 (d, *J* = 8.8 Hz, 2H), 7.44-7.42 (m, 1H), 7.29-7.26 (m, 1H), 6.93-6.85 (m, 4H), 6.80 (s, 1H), 6.58 (s, 1H), 4.52 (s, 2H), 3.99 (s, 6H), 3.89 (s, 3H), 3.82 (s, 3H), 3.81 (s, 2H), 3.49-3.44 (m, 2H), 2.76-2.72 (m, 4H), 1.97-1.94 (m, 2H), 1.16 (t, *J* = 7.2 Hz, 3H); ^{13}C NMR (100 MHz, $CDCl_3$) δ 177.1, 167.4, 160.7, 159.5, 157.9, 157.6, 154.3, 152.4, 140.2, 131.3, 128.9, 127.6 (2C), 124.7, 120.2, 114.8 (2C), 112.7, 110.4, 107.2, 96.2, 67.0, 62.1, 61.5, 56.2, 55.1, 51.9, 51.8, 47.1, 39.1, 24.8, 10.4; MS (ESI) m/z 591.3 $[M + H]^+$.

*4.1.6.9.N-(4-(benzyl(methyl)amino)butyl)-2-(4-(5,6,7-trimethoxy-4-oxo-4H-chromen-2-yl)phenoxy)acetamide (**T-9**).* Light yellow oil. Yield 46.2%; Purity: 97.7% (by HPLC); ^{1}H NMR (400 MHz, $CDCl_3$) δ 7.84 (d, *J* = 8.8 Hz, 2H), 7.32-7.24 (m, 5H), 7.01 (d, *J* = 8.8 Hz), 6.91 (brs, 1H), 6.79 (s, 1H), 6.59 (s, 1H), 4.56 (s, 2H), 3.99 (s, 3H), 3.98 (s, 3H), 3.92 (s, 3H), 3.53 (s, 2H), 3.39-3.35 (m, 2H), 2.46-2.42 (m, 2H), 2.21 (s, 3H), 1.63-1.59 (m, 4H); ^{13}C NMR (100 MHz, $CDCl_3$) δ 177.1, 167.4, 160.5, 159.4, 157.6, 154.3, 152.4, 140.2, 138.1, 129.1 (2C), 128.2 (2C), 127.7 (2C), 127.1, 125.1, 115.0 (2C), 112.7, 107.3, 96.1, 67.3, 62.1, 62.0, 61.4, 56.5, 56.2, 41.9, 38.8, 27.1, 24.4; MS (ESI) m/z 561.3 $[M + H]^+$.

*4.1.6.10.N-(4-(benzyl(ethyl)amino)butyl)-2-(4-(5,6,7-trimethoxy-4-oxo-4H-chromen-2-yl)phenoxy)acetamide (**T-10**).* Light yellow oil. Yield 51.2%; Purity: 96.9% (by HPLC); ^{1}H NMR (400 MHz, $CDCl_3$) δ 7.85 (d, *J* = 9.2 Hz, 2H), 7.31-7.23 (m, 5H), 7.02 (d, *J* = 8.8 Hz, 2H), 6.79 (s, 1H), 6.70 (brs, 1H), 6.59 (s, 1H), 4.55 (s, 2H), 3.99 (s, 6H), 3.92 (s, 3H), 3.57 (s, 2H), 3.37-3.32 (m, 2H), 2.55-2.46 (m, 4H), 1.58-1.54 (m, 4H), 1.05 (t, *J* = 6.8 Hz, 3H); ^{13}C NMR (100 MHz, $CDCl_3$) δ 177.0, 167.3, 160.4, 159.4, 157.5, 154.3, 152.3, 140.2, 138.8, 128.8 (2C), 128.1 (2C), 127.7 (2C), 126.8, 125.0, 114.9 (2C), 112.6, 107.2, 96.1, 67.2, 62.0, 61.4, 57.7, 56.2, 52.3, 47.0, 38.8, 27.2, 24.1, 11.2;

MS (ESI) m/z 575.3 $[M + H]^+$.

*4.1.6.11.N-(4-((2-methoxybenzyl)(methyl)amino)butyl)-2-(4-(5,6,7-trimethoxy-4-oxo-4H-chromen-2-yl)phenoxy)acetamide (**T-11**).* Light yellow oil. Yield 47.4%; Purity: 98.6% (by HPLC); ^{1}H NMR (400 MHz, $CDCl_3$) δ 7.83 (d, *J* = 9.2 Hz, 2H), 7.36 (d, *J* = 6.8 Hz, 1H), 7.29 (t, *J* = 7.6 Hz, 1H), 7.21 (brs, 1H), 6.99 (d, *J* = 8.8 Hz, 2H), 6.95 (t, *J* = 7.6 Hz, 1H), 6.88 (d, *J* = 8.0 Hz, 1H), 6.80 (s, 1H), 6.58 (s, 1H), 4.55 (s, 2H), 3.99 (s, 6H), 3.93 (s, 3H), 3.84 (s, 3H), 3.69 (s, 2H), 3.40 (q, J_1 = 12.0 Hz, J_2 = 6.4 Hz, 2H), 2.62-2.59 (m, 2H), 2.31 (s, 3H), 1.67-1.63 (m, 4H); ^{13}C NMR (100 MHz, $CDCl_3$) δ 177.1, 167.4, 160.5, 159.5, 157.8, 157.6, 154.3, 152.3, 140.2, 131.3, 128.9, 127.7 (2C), 124.9, 120.2, 114.9 (2C), 112.6, 110.4, 107.2, 96.1, 67.2, 62.1, 61.4, 56.6, 56.2, 55.2, 55.0, 41.7, 38.6, 26.9, 23.9; MS (ESI) m/z 591.3 $[M + H]^+$.

*4.1.6.12.N-(4-(ethyl(2-methoxybenzyl)amino)butyl)-2-(4-(5,6,7-trimethoxy-4-oxo-4H-chromen-2-yl)phenoxy)acetamide (**T-12**).* Light yellow oil. Yield 53.1% ; Purity: 98.2% (by HPLC); ^{1}H NMR (400 MHz, $CDCl_3$) δ 7.83 (d, *J* = 8.8 Hz, 2H), 7.62 (d, *J* = 7.2 Hz, 1H), 7.53 (brs, 1H), 7.38 (t, *J* = 8.0 Hz, 1H), 7.13 (d, *J* = 8.4 Hz, 2H), 7.01 (t, *J* = 7.2 Hz, 1H), 6.92 (d, *J* = 8.4 Hz, 1H), 6.78 (s, 1H), 6.57 (s, 1H), 4.58 (s, 2H), 4.20 (s, 2H), 3.98 (s, 6H), 3.91 (s, 3H), 3.87 (s, 3H), 3.41 (q, J_1 = 12 Hz, J_2 = 5.6 Hz, 2H), 3.04-2.94 (m, 4H), 1.98-1.93 (m, 2H), 1.68-1.62 (m, 2H), 1.39 (t, *J* = 7.2 Hz, 3H); ^{13}C NMR (100 MHz, $CDCl_3$) δ 177.1, 168.0, 160.7, 159.7, 158.0, 157.6, 154.4, 152.4, 140.2, 133.0, 131.4, 127.7, 124.8, 121.2, 117.5, 115.2, 112.7, 110.9, 107.2, 96.2, 67.1, 62.1, 61.5, 56.3, 55.5, 51.2, 49.9, 46.8, 37.5, 29.6, 26.4, 8.7; MS (ESI) m/z 605.3 $[M + H]^+$.

*4.1.6.13.N-(6-(benzyl(methyl)amino)hexyl)-2-(4-(5,6,7-trimethoxy-4-oxo-4H-chromen-2-yl)phenoxy)acetamide (**T-13**).* Light yellow oil. Yield 41.3%; Purity: 97.4% (by HPLC); ^{1}H NMR (400 MHz, $CDCl_3$) δ 7.86 (d, *J* = 9.2 Hz, 2H), 7.32-7.24 (m, 5H), 7.04 (d, *J* = 8.8 Hz, 2H), 6.80 (s, 1H), 6.60 (s, 1H), 6.55 (brs, 1H), 4.56 (s, 2H), 3.99 (s, 6H), 3.92 (s, 3H), 3.51 (s, 2H), 3.38-3.33 (m, 2H), 2.39-2.37 (m, 2H), 2.21 (s, 3H), 1.59-1.52 (m, 4H), 1.35-1.31 (m, 4H); ^{13}C NMR (100 MHz, $CDCl_3$) δ 177.0, 167.2, 160.5, 159.4, 157.6, 154.3, 152.4, 140.2, 138.7, 129.0 (2C), 128.1 (2C), 127.7 (2C), 126.9, 125.2, 115.0 (2C), 112.7, 107.3, 96.1, 67.3, 62.1, 61.4, 57.1, 56.2, 42.0, 39.0, 29.4, 27.1, 26.9, 26.6; MS (ESI) m/z 589.4 $[M + H]^+$.

*4.1.6.14.N-(6-(benzyl(ethyl)amino)hexyl)-2-(4-(5,6,7-trimethoxy-4-oxo-4H-chromen-2-yl)phenoxy)acetamide (**T-14**).* Light yellow oil. Yield 41.3%; Purity: 97.1% (by HPLC); ^{1}H NMR (400 MHz, $CDCl_3$) δ 7.86 (d, *J* = 8.4 Hz, 2H), 7.39-7.25 (m, 5H), 7.05 (d, *J* = 9.2 Hz, 2H), 6.80 (s, 1H), 6.60 (s,

1H), 6.58 (brs, 1H), 4.56 (s, 2H), 3.99 (s, 6H), 3.92 (s, 3H), 3.68 (s, 2H), 3.37-3.32 (m, 2H), 2.63-2.50 (m, 4H), 1.59-1.52 (m, 4H), 1.33-1.29 (m, 4H), 1.11 (t, *J* = 6.8 Hz, 3H); ^{13}C NMR (100 MHz, $CDCl_3$) δ 177.1, 167.3, 160.5, 159.4, 157.7, 154.4, 152.5, 140.3, 138.2, 129.3 (2C), 128.3 (2C), 127.8 (2C), 127.4, 125.3, 115.1 (2C), 112.8, 107.5, 96.2, 67.3, 62.2, 61.5, 57.5, 56.3, 52.6, 47.0, 39.0, 29.7 (2C), 29.4, 26.8, 26.5; MS (ESI) m/z 603.4 $[M + H]^+$.

*4.1.6.15.N-(6-((2-methoxybenzyl)(methyl)amino)hexyl)-2-(4-(5,6,7-trimethoxy-4-oxo-4H-chromen-2-yl)phenoxy)acetamide (**T-15**).* Light yellow oil. Yield 47.4%; Purity: 98.3% (by HPLC); ^{1}H NMR (400 MHz, $CDCl_3$) δ 7.85 (d, *J* = 8.8 Hz, 2H), 7.48 (d, *J* = 8.8 Hz, 1H), 7.36 (t, *J* = 8.0 Hz, 1H), 7.05 (d, *J* = 8.8 Hz, 2H), 6.98 (t, *J* = 7.2 Hz, 1H), 6.91 (d, *J* = 8.0 Hz, 1H), 6.80 (brs, 1H), 6.79 (s, 1H), 6.59 (s, 1H), 4.55 (s, 2H), 4.06 (s, 2H), 3.97 (s, 6H), 3.90 (s, 3H), 3.84 (s, 3H), 3.34 (q, J_1 = 13.2 Hz, J_2 = 6.4 Hz, 2H), 2.82-2.76 (m, 2H), 2.53 (s, 3H), 1.81-1.78 (m, 2H), 1.58-1.54 (m, 2H), 1.35-1.32 (m, 4H); ^{13}C NMR (100 MHz, $CDCl_3$) δ 177.1, 167.4, 160.5, 159.4, 158.0, 157.6, 154.3, 152.3, 140.2, 132.6, 130.6, 127.7 (2C), 124.9, 120.8, 115.0 (2C), 112.6, 110.7, 107.1, 96.2, 67.1, 62.1, 61.4, 56.2, 55.5, 55.4, 53.3, 39.8, 38.7, 29.0, 26.3, 26.1, 24.6; MS (ESI) m/z 619.3 $[M + H]^+$.

*4.1.6.16.N-(6-(ethyl(2-methoxybenzyl)amino)hexyl)-2-(4-(5,6,7-trimethoxy-4-oxo-4H-chromen-2-yl)phenoxy)acetamide (**T-16**).* Light yellow oil. Yield 48.3%; Purity: 98.7% (by HPLC); ^{1}H NMR (400 MHz, $CDCl_3$) δ 7.86 (d, *J* = 8.8 Hz, 2H), 7.54 (d, *J* = 7.2 Hz, 1H), 7.30 (t, *J* = 7.2 Hz, 1H), 7.06 (d, *J* = 8.8 Hz, 2H), 6.97 (t, *J* = 7.2 Hz, 1H), 6.89 (d, *J* = 8.0 Hz, 1H), 6.81 (s, 1H), 6.66 (brs, 1H), 6.60 (s, 1H), 4.56 (s, 2H), 3.99 (s, 6H), 3.92 (s, 3H), 3.85 (s, 2H), 3.84 (s, 3H), 3.35 (q, J_1 = 13.2 Hz, J_2 = 6.8 Hz, 2H), 2.77-2.63 (m, 4H), 1.69-1.66 (m, 2H), 1.59-1.54 (m, 2H), 1.34-1.32 (m, 4H), 1.21 (t, *J* = 6.8 Hz, 3H); ^{13}C NMR (100 MHz, $CDCl_3$) δ 177.0, 167.3, 160.5, 159.4, 157.7, 157.6, 154.3, 152.4, 140.2, 131.5, 129.4, 127.7 (2C), 125.1, 120.6, 115.0 (2C), 112.6, 110.4, 107.2, 96.2, 67.2, 62.1, 61.4, 56.2, 55.3, 52.3, 50.5, 47.2, 38.8, 29.2, 26.6, 26.3, 25.2, 10.3; MS (ESI) m/z 633.4 $[M + H]^+$.

*4.1.6.17.2-(4-(5-Hydroxy-6,7-dimethoxy-4-oxo-4H-chromen-2-yl)phenoxy)-N-(2-((2-methoxybenzyl)(methyl)amino)ethyl)acetamide (**T-17**).* Light yellow oil. Yield 43.2%; Purity: 98.2% (by HPLC); ^{1}H NMR (400 MHz, $CDCl_3$) δ 12.73 (s, 1H), 7.83 (d, *J* = 8.8 Hz, 2H), 7.53 (brs, 1H), 7.33 (d, *J* = 7.6 Hz, 1H), 7.22 (t, *J* = 7.2 Hz, 1H), 7.06 (d, *J* = 8.8 Hz, 2H), 6.89-6.84 (m, 2H), 6.80 (s, 1H), 6.56 (s, 1H), 4.54 (s, 2H), 4.00 (s, 3H), 3.84 (s, 3H), 3.82 (s, 3H), 3.65 (s, 2H), 3.53-3.51 (m, 2H), 2.68 (t, *J* = 7.2 Hz, 2H), 2.29 (s, 3H); ^{13}C NMR (100 MHz, $CDCl_3$) δ 182.6, 167.3, 163.4, 160.1, 158.9, 157.8, 153.5, 152.8, 132.5, 130.7, 127.9 (2C), 124.6, 120.4, 115.2 (2C), 110.3, 106.1, 104.3, 90.5, 67.3, 60.8, 56.28,

55.9, 55.0, 54.9, 41.8, 36.3; MS (ESI) m/z 549.2 $[M + H]^+$.

*4.1.6.18.N-(2-(ethyl(2-methoxybenzyl)amino)ethyl)-2-(4-(5-hydroxy-6,7-dimethoxy-4-oxo-4H-chromen-2-yl)phenoxy)acetamide (**T-18**).* Light yellow oil. Yield 49.1%; Purity: 97.8% (by HPLC); ^{1}H NMR (400 MHz, $CDCl_3$) δ 12.73 (s, 1H), 7.86 (d, *J* = 8.8 Hz, 2H), 7.37 (brs, 1H), 7.30 (d, *J* = 6.4 Hz, 1H), 7.23 (t, *J* = 7.2 Hz, 1H), 7.03 (d, *J* = 8.4 Hz, 2H), 6.89-6.84 (m, 2H), 6.60 (s, 1H), 6.56 (s, 1H), 4.54 (s, 2H), 3.98 (s, 3H), 3.93 (s, 3H), 3.79 (s, 3H), 3.60 (s, 2H), 3.45-3.41 (m, 2H), 2.63 (t, *J* = 7.2 Hz, 2H), 2.51 (m, 2H), 0.98 (t, *J* = 7.2Hz, 3H); ^{13}C NMR (100 MHz, $CDCl_3$) δ 182.6, 167.0, 163.4, 160.1, 158.7, 157.7, 153.1, 153.0, 132.5, 130.1, 128.1 (2C), 124.8, 120.2, 115.1 (2C), 110.3. 106.1, 104.5, 90.5, 67.3, 60.8, 56.3, 55.2, 51.6, 51.2, 47.5, 36.2, 11.8; MS (ESI) m/z 563.3 $[M + H]^+$.

*4.1.6.19.2-(4-(5-Hydroxy-6,7-dimethoxy-4-oxo-4H-chromen-2-yl)phenoxy)-N-(3-((2-methoxybenzyl)(methyl)amino)propyl)acetamide (**T-19**).* Light yellow oil. Yield 47.1%; Purity: 98.1 % (by HPLC); ^{1}H NMR (400 MHz, $CDCl_3$) δ 12.73 (s, 1H), 8.40 (brs, 1H), 7.77 (d, *J* = 8.4 Hz, 2H), 7.29-7.26 (m, 2H), 6.92 (t, *J* = 7.2 Hz), 6.86 (d, *J* = 8.4 Hz, 2H), 6.79-6.74 (m, 2H), 6.57 (s, 1H), 6.55 (s, 1H), 4.53 (s, 2H), 3.98 (s, 3H), 3.93 (s, 3H), 3.81 (s, 3H), 3.60 (s, 2H), 3.50-3.43 (m, 2H), 2.63-2.59 (m, 2H), 2.16 (s, 3H), 1.81-1.77 (m, 2H); ^{13}C NMR (100 MHz, $CDCl_3$) δ 182.5, 167.1, 163.4, 160.1, 158.7, 158.0, 153.1, 152.9, 132.2, 132.5, 131.3, 128.9, 127.9 (2C), 124.4, 120.1, 114.9 (2C), 110.4. 106.0, 104.3, 90.5, 67.1, 60.7, 56.8, 56.6, 56.2, 55.0, 41.3, 39.3, 25.1; MS (ESI) m/z 563.3 $[M + H]^+$.

*4.1.6.20.N-(3-(ethyl(2-methoxybenzyl)amino)propyl)-2-(4-(5-hydroxy-6,7-dimethoxy-4-oxo-4H-chromen-2-yl)phenoxy)acetamide (**T-20**).* Light yellow oil. Yield 43.1%; Purity: 98.5 % (by HPLC); ^{1}H NMR (400 MHz, $CDCl_3$) δ 12.73 (s, 1H), 8.28 (brs, 1H), 7.79 (d, *J* = 8.8 Hz, 2H), 7.38-7.35 (m, 1H), 7.27-7.25 (m, 1H), 6.92-6.82 (m, 4H), 6.57 (s, 1H), 6.54 (s, 1H), 4.51 (s, 2H), 3.97 (s, 3H), 3.92 (s, 3H), 3.80 (s, 3H), 3.74 (s, 2H), 3.48-3.44 (m, 2H), 2.69-2.62 (m, 4H), 1.89-1.86 (m, 2H), 1.09 (t, *J* = 6.8 Hz, 3H); ^{13}C NMR (100 MHz, $CDCl_3$) δ 182.4, 167.2, 163.4, 159.9, 158.6, 157.9, 153.0, 152.8, 132.4, 131.3, 129.0, 127.9 (2C), 124.3, 120.2, 114.9 (2C), 110.3, 105.9, 104.2, 90.4, 67.0, 60.7, 56.2, 55.0, 51.8, 51.7, 47.1, 39.0, 24.7, 10.3; MS (ESI) m/z 577.3 $[M + H]^+$.

*4.1.6.21.2-(4-(5-Hydroxy-6,7-dimethoxy-4-oxo-4H-chromen-2-yl)phenoxy)-N-(4-((2-methoxybenzyl)(methyl)amino)butyl)acetamide (**T-21**).* Light yellow oil. Yield 47.4%; Purity: 98.9 % (by HPLC); ^{1}H NMR (400 MHz, $CDCl_3$) δ 12.73 (s, 1H), 7.85 (d, *J* = 9.2 Hz, 2H), 7.41 (brs, 1H), 7.34-7.27 (m, 2H), 7.06-7.02 (m, 2H), 6.97 (t, *J* = 6.8 Hz, 1H), 6.90 (d, *J* = 8.4 Hz, 1H), 6.58 (s, 1H), 6.55 (s, 1H), 4.57 (s, 2H), 3.97 (s, 3H), 3.93 (s, 3H), 3.84 (s, 3H), 3.83 (s, 2H), 3.41 (m, 2H), 2.72-2.69 (m, 2H), 2.41 (s,

3H), 1.79-1.65 (m, 4H); ^{13}C NMR (100 MHz, $CDCl_3$) δ 182.6, 167.5, 163.4, 160.0, 158.7, 157.9, 153.2, 153.0, 132.6, 131.9, 129.8, 128.1 (2C), 124.7, 120.6, 115.2 (2C), 110.6. 106.1, 104.5, 90.5, 67.3, 60.9, 56.3, 55.4, 54.6, 54.5, 41.2, 38.3, 26.7, 23.3; MS (ESI) m/z 577.3 $[M + H]^+$.

*4.1.6.22.N-(4-(ethyl(2-methoxybenzyl)amino)butyl)-2-(4-(5-hydroxy-6,7-dimethoxy-4-oxo-4H-chromen-2-yl)phenoxy)acetamide (**T-22**).* Light yellow oil. Yield 44.3% yield, Purity: 98.8 % (by HPLC); ^{1}H NMR (400 MHz, $CDCl_3$) δ 12.73 (s, 1H), 7.86 (d, *J* = 8.8 Hz, 2H), 7.50 (m, *J* = 7.2 Hz, 1H), 7.30 (t, *J* = 8.0 Hz, 1H), 7.20 (brs, 1H), 7.09 (d, *J* = 8.8Hz, 2H), 6.97 (t, *J* = 7.2 Hz, 1H), 6.89 (d, *J* = 8.0 Hz, 1H), 6.58 (s, 1H), 6.55 (s, 1H), 4.57 (s, 2H), 3.98 (s, 3H), 3.93 (s, 3H), 3.88 (s, 2H), 3.84 (s, 3H), 3.41-3.36 (m, 2H), 2.77-2.73 (m, 4H), 1.77-1.75 (m, 2H), 1.66-1.61 (m, 2H), 1.22 (t, *J* = 6.8 Hz, 3H); ^{13}C NMR (100 MHz, $CDCl_3$) δ 182.4, 167.4, 163.4, 160.0, 158.6, 157.7, 153.0, 152.8, 132.4, 131.36, 129.4, 128.0 (2C), 124.5, 120.5, 115.1 (2C), 110.4. 105.9, 104.2, 90.5, 67.2, 60.7, 56.2, 55.3, 52.0, 50.6, 47.2, 38.3, 26.8, 23.0, 10.2; MS (ESI) m/z 591.3 $[M + H]^+$.

*4.1.6.23.2-(4-(5-Hydroxy-6,7-dimethoxy-4-oxo-4H-chromen-2-yl)phenoxy)-N-(6-((2-methoxybenzyl)(methyl)amino)hexyl)acetamide (**T-23**).* Light yellow oil. Yield 48.1%; Purity: 97.4 % (by HPLC); ^{1}H NMR (400 MHz, $CDCl_3$) δ 12.71 (s, 1H), 7.88 (d, *J* = 8.8 Hz, 2H), 7.53 (d, J = 7.2 Hz, 1H), 7.39 (t, *J* = 7.2 Hz, 1H), 7.09 (d, *J* = 8.8 Hz, 2H), 7.01 (t, *J* = 7.6 Hz, 1H), 6.94 (d, *J* = 8.0 Hz, 1H), 6.81 (brs, 1H), 6.61 (s, 1H), 6.56 (s, 1H), 4.56 (s, 2H), 4.15 (s, 2H), 3.98 (s, 3H), 3.93 (s, 3H), 3.87 (s, 3H), 3.37 (q, J_1 = 12.8 Hz, J_2 = 6.4 Hz, 2H), 2.86 (t, *J* = 7.2 Hz, 2H), 2.58 (s, 3H), 1.86-1.83 (m, 2H), 1.60-1.57 (m, 2H), 1.39-1.36 (m, 4H); ^{13}C NMR (100 MHz, $CDCl_3$) δ 182.4, 167.3, 163.3, 159.9, 158.7, 158.0, 153.0, 152.8, 132.9, 132.4, 130.9, 128.0 (2C), 124.6, 120.9, 118.6, 115.1 (2C), 110.7, 105.9, 104.2, 90.5, 67.2, 60.7, 56.2, 55.4, 55.2, 52.9, 39.3, 38.7, 29.0, 26.2, 26.0, 24.3, 22.6; MS (ESI) m/z 605.3 $[M + H]^+$.

*4.1.6.24.N-(6-(ethyl(2-methoxybenzyl)amino)hexyl)-2-(4-(5-hydroxy-6,7-dimethoxy-4-oxo-4H-chromen-2-yl)phenoxy)acetamide (**T-24**).* Light yellow oil. Yield 48.1%; Purity: 97.1 % (by HPLC); ^{1}H NMR (400 MHz, $CDCl_3$) δ 12.73 (s, 1H), 7.89 (d, *J* = 8.8 Hz, 2H), 7.65 (d, *J* = 6.4 Hz, 1H), 7.37 (t, *J* = 7.2 Hz, 1H), 7.09 (d, *J* = 8.8 Hz, 2H), 7.02 (t, *J* = 7.2 Hz, 1H), 6.93 (d, *J* = 8.0 Hz, 1H), 6.78 (brs, 1H), 6.61 (s, 1H), 6.57 (s, 1H), 4.58 (s, 2H), 4.16 (s, 2H), 3.98 (s, 3H), 3.93 (s, 3H), 3.87 (s, 3H), 3.39-3.33 (m, 2H), 2.96-2.84 (m, 4H), 1.65-1.58 (m, 6H), 1.38-1.36 (m, 5H); MS (ESI) m/z 619.3 $[M + H]^+$.

4.2. Biological evaluation.

4.2.1. Inhibition experiments of AChE and BuChE.

The determination of AChE and BuChE inhibitory capacity of the compounds were tested by Ellman assay with slight modification, using AChE from 5% rat cortex homogenate or purified AChE from *electric eel* (Sigma-Aldrich Co.) or BuChE from rat serum [22,23]. The brain homogenate was pre-incubated for 5 min with tetraisopropyl pyrophosphoramide (*iso*-OMPA, selective inhibitor of BuChE, 4.0 mmol/L) (Sigma-Aldrich Co.) before use. For rat AChE or BuChE inhibition assays, a reaction mixture (100 μL) containing acetylthiocholine iodide (1 mmol/L, 30 μL) (J&K Scientific) or butyrylthiocholine iodide (1 mmol/L, 30 μL) (TCI Shanghai Development), phosphate-buffered solution (0.1 mmol/L, pH = 7.4, 40 μL), 5% homogenate or 25% serum (10 μL) and different concentrations (< 1% DMSO) of test compounds (20 μL) was incubated at 37°C for 15 min. Then 5,5'-dithiobis-2-nitrobenzoic acid (DTNB, 0.2%, 30 μL) (J&K Scientific) was added. The activities were determined by using a Varioskan Flash Multimode Reader (Thermo Scientific) at 405 nm. For electric eel AChE and human AChE inhibition assay, *Ee*AChE or *Hu*AChE (0.05 U/mL, final concentration) was used and the assay was carried out in a phosphate buffer (0.1 mmol/L, pH=8.0). Changes in absorbance were detected at 412 nm. The other procedure was the same as described above. Compounds inhibiting AChE or BuChE activity would reduce the color generation. Thus, IC_{50} values were calculated as the concentration of compound that produces 50% AChE or BuChE activity inhibition. Data presented were the average of three independent experiments ± SD

4.2.2. Kinetic characterization of AChE inhibition.

Kinetic characterization of AChE inhibition was performed based on a reported method using purified AChE from *electric eel* (*Ee*AChE) [35]. The assay solution (100 μL) consists of 0.1 M phosphate buffer (pH 8.0), with the addition of 30 μL of 0.2% DTNB, 10 μL of 0.5 units/mL *Ee*AChE, and 20 μL of substrate (ATCh). Three different concentrations of inhibitors were added to the assay solution and pre-incubated for 15 min at 37 °C with the *Ee*AChE followed by the addition of substrate in different concentrations (0.1-0.4 mM). Kinetic characterization of the hydrolysis of ATCh catalyzed by *Ee*AChE was done spectrometrically at 412 nm. The parallel control experiments were performed without inhibitor in the assay. The plots were assessed by a weighted least square analysis that assumed the variance of *V* to be a constant percentage of *V* for the entire data set. Slopes

of these reciprocal plots were then plotted against the concentration of the inhibitors in a weighted analysis.

4.2.3. Molecular docking.

The crystal structure of AChE complexed with donepezil (code ID: *1EVE*) was obtained from the Protein Data Bank after eliminating the original inhibitors and water molecules [26]. The 3D Structure of **T-22** was built and performed geometry optimization by molecular mechanics. After addition of Gasteiger charges, removal of hydrogen atoms, addition of their atomic charges to skeleton atoms, and the assignment of proper atomic types, the further preparation of the inhibitor was accomplished. Autotors was then used to define the rotatable bonds in the ligands. Docking studies were performed using the AUTODOCK 4.2 program. By using Autodock Tools (ADT; version 1.5.6), polar hydrogen atoms were added to amino acid residues, and Gasteiger charges were assigned to all atoms of the enzyme. The resulting enzyme structure was used as an input for the AUTOGRID program. AUTOGRID performed a pre-calculated atomic affinity grid maps for each atom type in the ligand, plus an electrostatics map and a separate desolvation map presented in the substrate molecule. All maps were calculated with 0.375 Å spacing between grid points. The center of the grid box was placed at the center of donepezil with coordinates x = 2.023, y = 63.295, z = 67.062. The dimensions of the active site box were set at 50 × 50 × 50 Å. Flexible ligand docking was performed for the compounds. Each docked system was performed by 100 runs of the AUTODOCK search by the Lamarckian genetic algorithm (LGA). Other than the referred parameters above, the other parameters were accepted as default. A cluster analysis was performed on the docking results using a root mean square (RMS) tolerance of 1.0 and the lowest energy conformation of the highest populated cluster was selected for analysis. Graphic manipulations and visualizations were done by Autodock Tools or Discovery Studio 2.1 software.

4.2.4. Metal binding studies.

The metal binding studies were carried out in a Varioskan Flash Multimode Reader (Thermo Scientific) [27]. The UV absorption of the tested compound **T-22**, in the absence or presence of $CuCl_2$, $ZnCl_2$, $AlCl_3$ and $FeSO_4$ was recorded with wavelength ranging from 200 to 600 nm after incubating for 30 min in methanol at room temperature. The final volume of reaction mixture was 200 μL, and the final concentrations of tested compound and metals were 37.5 μM.

The stoichiometry of the compound-Cu^{2+} complex was determined by titrating the methanol

solution of tested compound with ascending of $CuCl_2$. The final concentration of tested compound was 37.5 μM, and the final concentration of Cu^{2+} ranged from 3.75 to 93.75 μM. The UV spectra was recorded and treated by numerical subtraction of $CuCl_2$ and tested compound at corresponding concentrations, plotted versus the mole fraction of tested compound.

4.2.5. Antioxidant activity assay.

The antioxidant activity was determined by the oxygen radical absorbance capacity fluorescein (ORAC-FL) assay [28,36]. 2,2'-Azobis(amidinopropane) dihydrochloride (AAPH) was purchased from Accela ChemBio Co., Ltd. 6-hydroxy-2,5,7,8-tetramethylchromane-2-carboxylic acid (trolox), and fluorescein (FL) were purchased from TCI (Shanghai) Development. All the assays were conducted with 75 mM phosphate buffer (pH 7.4), and the final reaction mixture was 200 μL. Antioxidant (20 μL) and fluorescein (120 μL, 150nM final concentration) were placed in the wells of a black 96-well plate. The mixture was pre-incubated for 15 min at 37 °C, and then AAPH solution (60 μL, 12 mM final concentration) was added rapidly using an autosampler. The plate was immediately placed in a Varioskan Flash Multimode Reader (Thermo Scientific) and the fluorescence recorded every minute for 90 min with excitation at 485 nm and emission at 535 nm. The plate was automatically shaken prior to each reading. Trolox was used as standard (1-8 μM, final concentration). A blank (FL + AAPH) using phosphate buffer instead of antioxidant and trolox calibration were carried out in each assay. The samples were measured at different concentration (1-10 μM). All the reaction mixture was prepared in duplicate, and at least three independent assays were performed for each sample. Antioxidant curves (fluorescence versus time) were normalized to the curve of the blank in the same assay, The ORAC-FL values were calculated as described in the reference, and the final results were in (μM Trolox equivalent)/(μM pure compound).

4.2.6. Effect of test compounds on self-induced $A\beta_{1-42}$ aggregation assay.

In order to investigate the self-induced $A\beta_{1-42}$ aggregation, a Thioflavin T-based flurometric assay was performed [29,30,37]. Thioflavin T was purchased from TCI (Shanghai) Development. Amyloid-β_{1-42} ($A\beta_{1-42}$), supplied as trifluoroacetate salt, was purchased from China Peptides Co., Ltd. 1,1,1,3,3,3-hexafluoro-2-propanol (HFIP) were purchased from Energy Chemical. Briefly, $A\beta_{1-42}$ was dissolved in HFIP (1 mg/mL) and incubated for 24h at room temperature, and solvent was evaporated. Then the HFIP pretreated $A\beta_{1-42}$ was re-solubilized in dry DMSO in order to have a stable stock solution of 200 μM and was kept at –80 °C. Solutions of tested compounds were

prepared in DMSO in 2.5 mM for storage and diluted with phosphate buffer solution (pH 7.4). Aβ_{1-42} (20 μL, 25 μM, final concentration) was incubated at 37 °C for 24 with or without 20 μL of test compounds at different concentrations ranging from 1-50 μM in 50 mM phosphate buffer solution (pH 7.4). To minimize evaporation effect the wells were sealed by a transparent heat-resistant plastic film. After incubated, 160 μL of 5 μM thioflavin T in 50 mM glycine-NaOH buffer (pH 8.5) was added. Each assay was run in triplicate. Fluorescence was measured by a Varioskan Flash Multimode Reader (Thermo Scientific) with excitation and emission wavelengths at 446 nm and 490 nm, respectively. The fluorescence intensities were compared and the percent inhibition due to the presence of the inhibitor was calculated by the expression $(1\text{-}IF_i/IF_c) \times 100$, in which IF_i and IF_c are the fluorescence intensities obtained for Aβ_{1-42} in the presence and absence of inhibitors after subtracting the background, respectively.

4.2.7. Inhibition of HuAChE-induced Aβ_{1-40} aggregation.

The thioflavin-T (ThT) fluorescence method was used as previously described [22,38,39]. HFIP pretreated Aβ_{1-40} (Sigma Co.) and tested compounds were dissolved in DMSO to obtain 2.3 mM and 1 mM solutions respectively. For the AChE-induced assay, Aliquots of 2 μL of Aβ_{1-40} were incubated for 24 h at room temperature in 0.215 mM sodium phosphate buffer (pH 8.0) at a final concentration of 230 μM. For co-incubations experiments, 16 μL of *Hu*AChE (final concentration of 2.3 μM, Aβ_{1-40}/AChE molar ration of 100:1) and AChE in the presence of 2 μL of the tested inhibitor (final concentration 100 μM) in 0.215 M sodium phosphate buffer (pH 8.0) solutions were added. Blanks containing Aβ_{1-40} alone, human AChE alone, and Aβ_{1-40} plus tested inhibitors in 0.215 mM sodium phosphate buffer (pH 8.0) were prepared. After incubation, 180 μL of 5 μM thioflavin T in 50 mM glycine-NaOH buffer (pH 8.5) was added. Each assay was run in triplicate. The detection method was the same as above. The percent inhibition of the AChE-induced aggregation due to the presence of the tested compound was calculated by the following formula: $100\text{-}IF_i/IF_c*100)$, where IF_i and IF_c were the fluorescence intensities obtained for Aβ plus AChE in the presence and in the absence of inhibitors, respectively, minus the fluorescence intensities due to the respectively blanks.

4.2.8. Effect of test compounds on metal-induced Aβ_{1-42} aggregation experiments and disaggregation by ThT method.

For the inhibition of Cu^{2+}-induced Aβ_{1-42} aggregation experiment [40]. HEPES buffer solutions (20 mM, pH 6.6) containing 150 μM NaCl were prepared with distilled water. Solutions of Cu^{2+} were

prepared from standards to concentration of 75 μM using the HEPES buffer at pH = 6.6. The A$\beta_{1\text{-}42}$ stock solution was diluted in HEPES buffer. The mixture of the peptide (20 μL, 25 μM, final concentration) and Cu^{2+} (20 μL, 25 μM, final concentration), was incubated at 37 °C for 24h with or without the tested compound at different concentrations (20 μL, 25 μM, final concentration). After incubated, 190 μL of 5 μM Thioflavin T in 50 mM glycine-NaOH buffer (pH 8.5) was added. Each assay was run in triplicate. The detection method was the same as that of self-induced A$\beta_{1\text{-}42}$ experiment.

For the disaggregation of copper-induced Aβ fibrils experiment, the A$\beta_{1\text{-}42}$ stock solution was diluted in HEPES buffer (20 mM, pH 6.6, 150 mM NaCl). The mixture of the A$\beta_{1\text{-}42}$ (20 μL, 25 μM, final concentration) with Cu^{2+} (20 μL, 25 μM, final concentration) was incubated 37 °C for 24 h. The tested compound (20 μL, 25 μM, final concentration) was then added and incubated at 37 °C for another 24 h. To minimize evaporation effect the wells were sealed by a transparent heat-resistant plastic film. After incubation, 190 μL of 5 μM thioflavin T in 50 mM glycine-NaOH buffer (pH 8.5) was added. Each assay was run in triplicate. The detection method was the same as above.

4.2.9. Studies of cytotoxic effects on SH-SY5Y (MTT assay) [41,42].

The human neuroblastoma SH-SY5Y cells were purchased from the American Type Culture Collection (ATCC). The cell line was maintained in Dulbecco's modified Eagle's medium (DMEM from GIBCO) containing 10% (v/v) fetal bovine serum (FBS, Hyclone), 100 U/ml penicillin, and 100 mg/ml streptomycin (Invitrogen). The cells were grown at 37 °C in a humidified atmosphere of 5% CO_2. For the MTT (3-(4,5-dimethylthiazol-2-yl)-2,5-diphenyltetrazolium bromide, Sigma-Aldrich) assay, SH-SY5Y cells were seeded in 96 well plate (4×10^4 cells in 100 μL per well). Then, the cells were incubated for 24 h at 37 °C. Due to the poor solubility of compound **T-12** and **T-22** in water or media, the final amount of DMSO used is 1% (v/v). On the consecutive day, the cells were treated with 25 μl MTT (5 mg/ml in PBS) for 4 h at 37 °C and then were lysed in a buffered solution containing *N*,*N*-dimethylformamide (pH 4.5, 50% (aq, v/v)) and sodium dodecyl sulfate (SDS, 20% (w/v)) overnight at room temperature in the dark. The absorbance (A590 nm) was measured using a Elx800 microplate reader (purched from Bio-Tek). % inhibition = $[1 - (A_{sample} / A_{control})] \times 100$.

4.2.10. Hydrogen peroxide induced PC12 cell injury. [26,31]

MTT reduction assay was determined with an *in vitro* toxicology assay. PC12 cells were propagated

in phenol red free Dulbecco's modified Eagle's medium (DMEM from GIBCO) containing 10% (v/v) fetal calf serum (FCS, Hyclone), 100 U/ml penicillin, and 100 mg/ml streptomycin (Invitrogen). The cells were grown at 37 °C in a humidified atmosphere of 5% CO_2. Neuronal PC12 cells were plated at a density of 10^5 cells/well on 96-well plates in 100 μl of DEME. The compounds **T-12** and **T-22** were dissolved with 2% DMSO first, and then diluted with phosphate-buffered saline (PBS). The cells were pre-incubated with compounds for 24 hours before H_2O_2 (100 μM) was added. The cells were treated with or without H_2O_2 for two hours, and then replaced with fresh DMEM medium. Assays for cell viability were performed 24 h after cultured at 37 °C in fresh medium. The cells were treated with 25 μl MTT (5 mg/ml in PBS) for 4 h at 37 °C and then were lysed in a buffered solution containing *N*,*N*-dimethylformamide (pH 4.5, 50% (aq, v/v)) and sodium dodecyl sulfate (SDS, 20% (w/v)) overnight at room temperature in the dark. The absorbance (A590 nm) was measured using Elx800 microplate reader (Bio-Tek). % inhibition = $[1-(A_{sample}/A_{control})]\times100$.

4.2.11. Step-down passive avoidance test.[23]

Materials and animals

Donepezil was purchased from Eisai China Inc. Scopolamine was purchase from J&K Scientific. Kunming mice at body weight of 18–22 g (six weeks old, either gender) were supplied by the Center of Experimental Animals of Sichuan Academy of Chinese Medicine Sciences (eligibility certification no. SCXK-Sichuan 2008-19). Mice were maintained under standard conditions with a 12 h:12 h light–dark cycle, a temperature and humidity controlled environment with access to food and water ad libitum. The mice were submitted to behavioral tests one day after 7 days of treatment with compounds.

Assay method

A modification of step-down passive avoidance test was used to assess learning and memory in mice. The apparatus consisted of a grid floor with a wooden block placed in the center. The block served as a shock free zone. The mice underwent two separate trials: a training trial and a test trial 24 h later. For training trial, mice were initially placed on the block and were given an electrical foot shock (0.5 mA, 2s) through the grid floor on stepping down. We used a total of 60 mice in the passive avoidance test with 10 mice were used per treatment. Compounds **T-22** (3.67, 7.33 and 22 mg/kg, *p.o.*) or donepezil (5.0 mg/kg, *p.o.*) as a positive control were orally given 1 h before each training trial. After 30 min, memory impairment was induced by administering scopolamine (3 mg/kg, *i.p.*). Twenty-four

hours after the training trial, mice were placed on the block and the time for the animal to step down was measured as latency time for test trial. An upper cut-off time was set at 300 s.

Statistical analysis

All data are expressed as mean ± SEM. Differences between groups were examined for statistical significance using one-way ANOVA with Student's *t* test. A *P* value less than 0.05 denoted the presence of a statistically significant difference.

Supporting Information Available:

^{1}HNMR and ^{13}CNMR spectra of some target compounds are available as supplementary material.

Acknowledgments

This work was supported in part by the Chinese National Natural Science Foundation (20872099), the Research Fund for the Doctoral Program of Higher Education (20110181110079) and the National Science and Technology Major Project on "Key New Drug Creation and Manufacturing Program"(2013ZX09301304-002).

References

[1] A. Samadi, C. de los Ríos, I. Bolea, M. Chioua, I. Iriepa, I. Moraleda, M. Bartolini, V. Andrisano, E. Gálvez, C. Valderas, M. Unzeta, J. Marco-Contelles, Multipotent MAO and cholinesterase inhibitors for the treatment of Alzheimer's disease: synthesis, pharmacological analysis and molecular modeling of heterocyclic substituted alkyl and cycloalkyl propargyl amine, Eur. J. Med. Chem. 52 (2012) 251-262.

[2] P. Martin, C. Adelina, K. Martin, G. Maëlenn, K. Maria, World Alzheimer report 2016: improving healthcare for people living with dementia: coverage, quality and costs now and in the future. (2016) 1-140. https://www.alz.co.uk/research/world-report-2016

[3] I. Silman, J.L. Sussman, Acetylcholinesterase: "classical" and "non-classical" functions and pharmacology, Curr. Opin. Pharmacol. 5 (2005) 293-302.

[4] D. Praticò, Oxidative stress hypothesis in Alzheimer's disease: a reappraisal, Trends Pharmacol. Sci. 29 (2008) 609-615.

[5] J. Hardy, D. J. Selkoe, The amyloid hypothesis of Alzheimer's disease: progress and problems on the road to therapeutics, Science 297 (2002) 353-356.

[6] E. Girard, V. Bernard, J. Minic, A. Chatonnet, E. Krejci, J. Molgó, Butyrylcholinesterase and the control of synaptic responses in acetylcholinesterase knockout mice, Life Sci. 80 (2007) 2380-2385.

[7] S. Schwarz, S.D. Lucas, S. Sommerwerk, R. Csuk, Amino derivatives of glycyrrhetinic acid as potential inhibitors of cholinesterase, Bioorg. Med. Chem. 22 (2014) 3370-3378.

[8] D.R. Liston, J.A. Nielsen, A. Villalobos, D. Chapin, S.B. Jones, S.T. Hubbard, I.A. Shalaby, A. Ramirez, D. Nason, W.F. White, Pharmacology of selective acetylcholinesterase inhibitors: implications for use in Alzheimer's disease, Eur. J. Pharmacol. 486 (2004) 9-17.

[9] P. Anand, B. Singh, A review on cholinesterase inhibitors for Alzheimer's disease. Arch. Pharm. Res. 36 (2013) 375-399.

[10] M.G. Savelieff, S. Lee, Y. Liu, M.H. Lim, Untangling amyloid-β, tau, and metals in Alzheimer's disease, ACS Chem. Biol. 8 (2013) 856-865.

[11] L. Sánchez, S. Madurga, T. Pukala, M. Vilaseca, C. López-Iglesias, C.V. Robinson, E. Giralt, N. Carulla, Aβ40 and Aβ42 amyloid fibrils exhibit distinct molecular recycling properties, J. Am. Chem. Soc. 133 (2011) 6505-6508.

[12] S.A. James, Q.I. Churches, M.D. de Jonge, I.E. Birchall, V. Streltsov, G. McColl, P.A. Adlard, D.J. Hare. Iron, copper, and zinc concentration in Aβ plaques in the APP/PS1 mouse model of Alzheimer's disease correlates with metal levels in the surrounding neuropil, ACS Chem. Neurosci. 8 (2017) 629-637.

[13] M. Soodi, A. Dashti, H. Hajimehdipoor, S. Akbari, N. Ataei, *Melissa officinalis* acidic fraction protects cultured cerebellar granule neurons against beta amyloid-induced apoptosis and oxidative stress, Cell J. 18(2017) 556-564.

[14] M.B. Franca, K.C. Lima, E.C.A. Eleutherio, Oxidative stress and amyloid toxicity: insights from yeast, J. Cell Biochem. 9999 (2016) 1-11.

[15] A. Agis-Torres, M. Sölhuber, M. Fernandez, J.M. Sanchez-Montero, Multi-target-directed ligands and other therapeutic strategies in the search of a real solution for Alzheimer's disease, Curr. Neuropharmacol. 12 (2014) 2-36.

[16] M. Bajda, N. Guzior, M. Ignasik, B. Malawska, Multi-target-directed ligands in Alzheimer's

disease treatment, Curr. Med. Chem. 18 (2011) 4949-4975.

[17] L.L. Guo, Z.Z. Guan, Y. Huang, Y.L. Wang, J.S. Shi, The neurotoxicity of β-amyloid peptide toward rat brain is associated with enhanced oxidative stress, inflammation and apoptosis, all of which can be attenuated by scutellarin. Exp. Toxicol. Pathol., 65 (2013), 579-584.

[18] H. Hong, G.Q. Liu, Protection against hydrogen peroxide-induced cytotoxicity in PC12 cells by scutellarin. Life Sci., 74 (2004) 2959-2973.

[19] J.T.T. Zhu, R.C.Y. Choi, J. Li, H.Q.H. Xie, C.W.C. Bi, A.W.H. Cheung, T.T.X. Dong, Z.Y. Jiang, J.J. Chen, K.W.K. Tsim, Estrogenic and neuroprotective properties of scutellarin from Erigeron breviscapus: a drug against postmenopausal symptoms and Alzheimer's disease. Planta Med. 75 (2009) 1489-1493.

[20] X.Y. Chen, L. Cui, X.T. Duan, B. Ma, D.F. Zhong, Pharmacokinetics and metabolism of the flavonoid scutellarin in humans after a single oral administration, Drug Metab. Dispos. 34 (2006) 1345-1352.

[21] M.L. Bolognesi, V. Andrison, M. Bartolini, R. Banzi, C. Melchiorre, Propidium-based polyamine ligands as potent inhibitors of acetylcholinesterase and acetylcholinesterase-induced amyloid-β aggregation, J. Med, Chem, 48 (2005) 24-27.

[22] Z.P. Sang, X.M. Qiang, Y. Li, W. Yuan, Q. Liu, Y.K. Shi, W. Ang, Y.F. Luo, Z.H. Tan, Y. Deng, Design, synthesis and evaluation of scutellarein-*O*-alkylamines as multifunctional agents for the treatment of Alzheimer's disease, Eur. J. Med. Chem. 94 (2015) 348-366.

[23] X.M. Qiang, Z.P. Sang, W. Yuan, Y. Li, Q. Liu, P. Bai, Y.K. Shi, W. Ang, Z.H. Tan, Y. Deng, Design, synthesis and evaluation of genistein-*O*-alkylbenzylamines as potential multifunctional agents for the treatment of Alzheimer's disease, Eur. J. Med. Chem. 76 (2014) 314-331.

[24] D. Alonso, I. Dorronsoro, L. Rubio; P. Muñoz, E. Garcia-Palomero, M. Del Monte, A. Bidon-Chanal, M. Orozco, F.J. Luque, A. Castro, M. Medina, A. Martinez, Donepezil-tacrine hybrid related derivatives as new dual binding site inhibitors of AChE. Bioorg. Med. Chem., 13 (2005) 6588-6597.

[25] S. Darvesh, D.A. Hopkins, C. Geula, Neurobiology of butyrylcholinesterase, Nat. Rev. Neurosci., 4 (2003) 131-138.

[26] Y. Li; X.M. Qiang; L. Luo; X. Yang; G.Y. Xiao; Q. Liu; J.C. Ai; Z.H. Tan; Y. Deng, Aurone Mannich base derivatives as promising multifunctional agents with acetylcholinesterase

inhibition, anti-β-amyloid aggragation and neuroprotective properties for the treatment of Alzheimer's disease, Eur. J. Med. Chem. 126 (2017) 762-775.

[27] M.Y. Wu, G. Esteban, S. Brogi, M. Shionoya, L. Wang, G. Campiani, M. Unzeta, T. Inokuchi, S. Butini, Donepezil-like multifunctional agents: design, synthesis, molecular modeling and biological evaluation, Eur. J. Med. Chem. 121 (2016) 864-879.

[28] Y. Li, X.M. Qiang, L. Luo, X. Yang, G.Y. Xiao, Y.X.Z. Zheng, Z.C. Cao, Z.P. Sang, F. Su, Y. Deng, Multitarget drug design strategy against Alzheimer's disease: Homoisoflavonoid Mannich base derivatives serve as acetylcholinesterase and monoamine oxidase B dual inhibitors with multifunctional properties, Bioorg. Med. Chem. 25 (2017) 714-726.

[29] X.M. Zha, D. Lamba, L.L. Zhang, Y.H. Lou, C.X. Xu, D. Kang, L. Chen, Y.G. Xu, L.Y. Zhang, A. De Simone, S. Samez, A. Pesaresi, J. Stojan, M.G. Lopez, J. Egea, V. Andrisano, M. Bartolini, Novel tacrine-benzofuran hybrids as potent multitarget-directed ligands for the treatment of Alzheimer's disease: design, synthesis, biological evaluation, and X-ray crystallography, J. Med. Chem. 59 (2016) 114-31.

[30] L. Huang, C.J. Lu, Y. Sun, F. Mao, Z.H. Luo, T. Su, H.L. Jiang, W.J. Shan, X.S. Li. Multitarget-diredted benzylideneindanone derivatives: anti-β-amyloid (Aβ) aggregation, antioxidant, metal chelation, and monoamine oxidase B (MAO-B) inhibition properties against Alzheimer's disease. J. Med. Chem. 55 (2012) 8483-8492.

[31] Z.P. Sang, Y. Li, X.M. Qiang, G.Y. Xiao, Q. Liu, Z.H. Tan, Y. Deng, Multifunctional scutellarin-rivastigmine hybrids with cholinergic, antioxidant, biometal chelating and neuroprotective properties for the treatment of Alzheimer's disease, Bioorg. Med. Chem. 23 (2015) 668-680.

[32] S.H. Kwon, H.K. Lee, J.A. Kim, S.I. Hong, H.C. Kim, T.H. Jo, Y.I. Park, C.K. Lee, Y.B. Kim, S.Y. Lee, C.G. Jang, Neuroprotective effects of chlorogenic acid on scopolamine-induced amnesia via anti-acetylcholinesterase and anti-oxidative activities in mice, Eur. J. Pharmacol. 649 (2010) 210-217.

[33] N. Cesari, C. Biancalani, C. Vergelli, V. Dal Piaz, A. Graziano, P. Biagini, C. Ghelardini, N. Galeotti, M.P. Giovannoni, Arylpiperazinylalkylpyridazinones and analogoues as potent and orally active antinociceptive agents: synthesis and studies on mechanism of action, J. Med. Chem., 49 (2006), 7826-7835.

[34] X.F. Kong, Z.Q. He, Y.N. Zhang, L.P. Mu, C.J. Liang, B. Chen, X.P. Jing, A. N. Cammidge, A mesogenic triphenylene-perylene-triphenylene triad. Org. Lett., 13 (2011) 764-767.

[35] T. Mohamed, P.P.N. Rao, 2,4-Disubstituted quinazolines as amyloid-β aggregation inhibitors with dual cholinesterase inhibition and antioxidant properties: Development and structure-activity relationship (SAR) studies, Eur. J. Med. Chem. 126 (2017) 823-843.

[36] A. Dávalos, C. Gómez-Cordovés, B. Bartolomé, Extending applicability of the oxygen radical absorbance capacity (ORAC-fluorescein) assay, J. Agric. Food Chem., 52 (2004) 48-54.

[37] P. Xu, M.K. Zhang, R. Sheng, Y.M Ma, Synthesis and biological evaluation of deferiprone-resveratrol hybrids as antioxidants, $A\beta_{1-42}$ aggregation inhibitors and metal-chelating agents for Alzheimer's disease. Eur. J. Med. Chem. 127 (2017) 174-186.

[38] P. Camps, X. Formosa, C. Galdeano, D. Muñoz-Torrero, L. Ramírez, E. Gómez, N. Isambert, R. Lavilla, A. Badia, M. V. Clos, M. Bartolini, F. Mancini, V. Andrisano, M.P. Arce, M. I. Rodriguez-Franco, O. Huertas, T. Dafni, F. J. Luque, Pyranl[3,2-c]quinoline-6-chlorotacrine hybrids as a novel family of acetylcholinesterase- and beta-amyloid-directed anti-Alzheimer compounds. J. Med. Chem. 52 (2009) 5365-5379.

[39] Y.X. Li, X.M. Qiang, Y. Li, X. Yang, L. Luo, G.Y. Xiao, Z.C. Cao, Z.H. Tan, Y. Deng. Pterostilbene-*O*-acetamidoalkylbenzylamines derivatives as novel dual inhibitors of cholinesterase with anti-β-amyloid aggregation and antioxidant properties for the treatment of Alzheimer's disease, Bioorg. Med. Chem. Lett. 26 (2016), 2035-2039.

[40] N. Jiang, S.Y. Li, S.S. Xie, Z.R. Li, K.D. Wang, X.B. Wang, L.Y. Kong. Design, synthesis and evaluation of multifunctional salphen derivatives for the treatment of Alzheimer's disease, Eur. J. Med. Chem. 87 (2014), 540-551.

[41] K. Seoposengwe, J.J. van Tonder, V. Steenkamp, In vitro neuroprotective potential of four medicinal plants against rotenone-induced toxicity in SH-SY5Y neuroblastoma cells, BMC complement. Altern. Med., 13 (2013), 353-364.

[42] X.K. Li, H. Wang, Z.Y. Lu, X.Y. Zheng, W. Ni, J. Zhu, Y. Fu, F.L. Lian, N.X. Zhang, J. Li, H.Y. Zhang, F. Mao, Development of multifunctional pyrimidinylthiourea derivatives as potential anti-Alzheimer agents, J. Med. Chem. 59 (2016) 8326-8344.

Figure, Scheme and Table Captions

Figure 1. Design strategy for the scutellarein-*O*-acetamidoalkylbenzylamines derivatives.

Figure 2. Kinetic study on the mechanism of *Ee*AChE inhibition by compound **T-22**. Merged Lineweaver-Burk reciprocal plots of AChE initial velocity with increasing substrate concentration (100-400 μM) in the absence or presence of **T-22**. Lines were derived from a weighted least-squares analysis of data points.

Figure 3. Representative compound **T-22** (colored by atom type) interacting with residues in the binding site of *Tc*AChE (PDB code: *1EVE*), highlighting the protein residues that participate in the main interaction with the inhibitor.

Figure 4. UV spectrum of compound **T-22** (37.5 μM in methanol) alone or in the presence of $CuCl_2$, $ZnCl_2$, $AlCl_3$ and $FeSO_4$ (37.5 μM for all metals in methanol).

Figure 5. Determination of the stoichiometry of complex-Cu^{2+} by using molar ratio method through titrating the methanol solution of compound **T-22** with ascending amounts of $CuCl_2$. The final concentration of tested compound was 37.5 μM, and the final concentration of Cu^{2+} ranged from 3.75 to 93.75 μM.

Figure 6. Inhibition of Cu^{2+}-induced aggregation by compounds **T-17~24** and curcumin. The thioflavin-T fluorescence method was used.

Figure 7. Effects of **T-12** and **T-22** on cell viability in human SH-SY5Y cells. Data are mean values ± SEM of three independent experiments.

Figure 8. Neuroprotective effect of compound **T-12** and **T-22** at the concentration of 1.0 μM and 10.0 μM on cell injury induced by hydrogen peroxide (H_2O_2, 100 μM) in PC12 cells.

Figure 9. Effects of compound **T-22** on scopolamine-induced memory deficit in the step-down passive avoidance test. Compounds **T-22** (3.67, 7.33 and 22.0 mg/kg, *p.o.*) or donepezil (5.0 mg/kg, *p.o.*) were orally given 1 h before treatment with scopolamine. After 30 min, the mice were treated with scopolamine (3 mg/kg, *i.p.*) and tested in the step-down passive avoidance. Values are expressed as the mean ± SEM (n=10). # $p < 0.05$ *vs* normal group. * $p < 0.05$ and ** $p < 0.01$ *vs* scopolamine-treated control group.

Scheme 1. Synthesis of scutellarein-*O*-acetamidoalkylbenzylamines derivatives **T-1~24**. *Reagents and conditions:* (a) $Br(CH_2)_nBr$, K_2CO_3, acetone, reflux, 7-8 h; (b) R_1R_2NH (**3a-d**)[21], K_2CO_3, CH_3CN, 65°C, 6-8 h; (c) $H_2NNH_2{\cdot}H_2O$, EtOH, reflux for 5 h; (d) *p*-MOM-O-PhCHO (**13**), 30% KOH, ethanol, at r.t. for 3 days; (e) 10% HCl, ethanol, 50°C, 4 h; (f) KI, *conc*.H_2SO_4, DMSO, 100°C, 3-5 h; (g)$AlCl_3$, anhydrous CH_3CN, 60°C, 1 h; (h) $BrCH_2COOC_2H_5$, K_2CO_3, anhydrous CH_3CN, 65°C, 8 h; (i) LiOH, THF/H_2O, reflux for 2 h, then 10% HCl; (j) EDCI, THF, at r.t. for over night.

Table 1. Inhibition of AChE and BuChE activity, and oxygen radicals absorbance capacity (ORAC, Trolox Equivalents) by compounds **T-1~24**, **16**, **17** and donepezil.

Table 2. Inhibition of self-induced Aβ_{1-42} aggregation, *Hu*AChE-induced Aβ_{1-40} aggregation, Cu^{2+}-induced Aβ_{1-42} aggregation and disaggregation of Cu^{2+}-induced Aβ_{1-42} aggregation by target compounds and reference compounds.

Highlights

- A series of novel scutellarein-*O*-acetamidoalkylbenzylamines were synthesized.
- Compound **T-22** exhibited good acetylcholinesterase inhibitory and antioxidant activity.
- Compound **T-22** exhibited excellent inhibitory effects on Aβ aggregation.
- Compound **T-22** markedly disassembled the Cu^{2+}-induced Aβ aggregation.
- **T-22** showed neuroprotective effects, low toxicity and reversed scopolamine-induced memory deficit in mice.